Project Report
ATC-248

Six-Sector Antenna for the GPS-Squitter En-Route Ground Station

M.L. Burrows

31 May 1996

Lincoln Laboratory
MASSACHUSETTS INSTITUTE OF TECHNOLOGY
LEXINGTON, MASSACHUSETTS

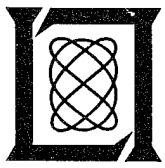

Prepared for the Federal Aviation Administration.
Document is available to the public through the National Technical Information Service, Springfield, Virginia 22161.

DISCLAIMER NOTICE

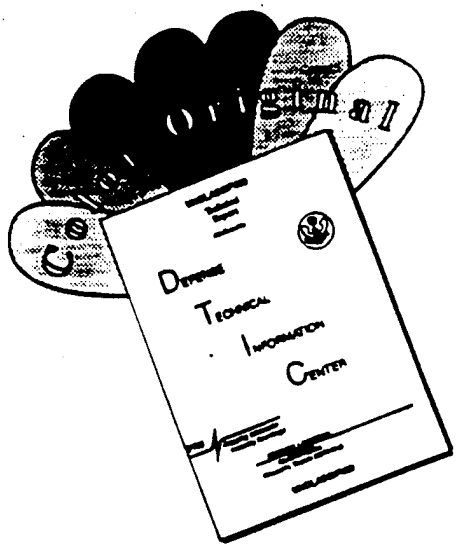

THIS DOCUMENT IS BEST QUALITY AVAILABLE. THE COPY FURNISHED TO DTIC CONTAINED A SIGNIFICANT NUMBER OF COLOR PAGES WHICH DO NOT REPRODUCE LEGIBLY ON BLACK AND WHITE MICROFICHE.

TECHNICAL REPORT STANDARD TITLE PAGE

1. Report No.	2. Government Accession No.	3. Recipient's Catalog No.
ATC-248		

4. Title and Subtitle	5. Report Date
Six-Sector Antenna for the GPS-Squitter En-Route Ground Station	31 May 1996
	6. Performing Organization Code

7. Author(s)	8. Performing Organization Report No.
Michael L. Burrows	ATC-248

9. Performing Organization Name and Address	10. Work Unit No. (TRAIS)
Lincoln Laboratory, MIT 244 Wood Street Lexington, MA 02173-9108	11. Contract or Grant No. DTFA01-93-Z-02012

12. Sponsoring Agency Name and Address	13. Type of Report and Period Covered
Department of Transportation Federal Aviation Administration Systems Research and Development Service Washington, DC 20591	Project Report/May 1996
	14. Sponsoring Agency Code

15. Supplementary Notes

This report is based on studies performed at Lincoln Laboratory, a center for research operated by Massachusetts Institute of Technology under Air Force Contract F19628-95-C-0002.

16. Abstract

A six-sector antenna for a pole-mounted GPS-Squitter en-route ground station was designed, built, and tested. The fan beam of each of the six sectors of the antenna covers a 60-degree azimuthal sector. Together, the six uniformly spaced, contiguous 60-degree sectors cover the complete 360 degrees of azimuth at the two Mode S frequencies: 1030 and 1090 MHz. When equipped with its receivers, the antenna achieves a maximum operational squitter reception range in excess of 200 nmi.

Physically, the antenna consists of six vertical 12-element linear arrays spaced uniformly around the circumference of an imaginary vertical circular cylinder and lying parallel to its axis. Six reflectors in the form of parabolic cylinders are mounted behind the linear arrays, one per array, to define the six separate sector beams. The complete radome-enclosed assembly is a cylinder 8 feet tall and 23 inches in diameter. It weights 250 pounds.

Antenna-range measurements of the antenna gain pattern verified that it meets its design goals. Reception tests in which the antenna was used to collect short squitters broadcast by air traffic being tracked by the MODSEF Mode S sensor demonstrated its system performance.

Three additional aspects of the antenna's use were demonstrated. These are, first, the emergency role of the antenna for direction finding in case GPS-derived position is temporarily lost, for which a potentially useful performance was exhibited; second, the application of the antenna to compiling performance statistics of the current population of aircraft transponders—an example, the distribution of transponder ERPs, is included here; and third, the use of the antenna on a buoy-mounted en-route "ground" station, including the effects on the link of buoy pitching sea-reflection multipath. The first two of these studies employed squitter data collected with the antenna; the last was a computer simulation.

17. Key Words	18. Distribution Statement
GPS-Squitter antenna aircraft surveillance ground station	This document is available to the public through the National Technical Information Service, Springfield, VA 22161.

19. Security Classif. (of this report)	20. Security Classif. (of this page)	21. No. of Pages	22. Price
Unclassified	Unclassified	72	

SUMMARY

A six-sector antenna for a pole-mounted GPS-Squitter en-route ground station was designed, built, and tested. The fan beam of each of the six sectors of the antenna covers a 60-degree azimuthal sector. Together, the six uniformly-spaced, contiguous 60-degree sectors cover the complete 360 degrees of azimuth at the two Mode S frequencies, 1030 and 1090 MHz. When equipped with its receivers, the antenna achieves a maximum operational squitter reception range in excess of 200 nmi.

Physically, the antenna consists of six vertical 12-element linear arrays spaced uniformly around the circumference of an imaginary vertical circular cylinder and lying parallel to its axis. Six reflectors in the form of parabolic cylinders are mounted behind the linear arrays, one per array, to define the six separate sector beams. The complete radome-enclosed assembly is a cylinder eight feet tall and 23 inches in diameter. It weighs 250 pounds.

Antenna-range measurements of the antenna gain pattern verified that it meets its design goals. Reception tests in which the antenna was used to collect short squitters broadcast by air traffic being tracked by the MODSEF Mode S sensor demonstrated its system performance.

Three additional aspects of the antenna's use were demonstrated. These are, first, the emergency role of the antenna for direction finding in case GPS-derived position is temporarily lost, for which a potentially useful performance was exhibited; second, the application of the antenna to compiling performance statistics of the current population of aircraft transponders — an example, the distribution of transponder ERPs, is included here; and third, the use of the antenna on a buoy-mounted en-route 'ground' station, including the effects on the link of buoy pitching and sea-reflection multipath. The first two of these studies employed squitter data collected with the antenna; the last was a computer simulation.

ACKNOWLEDGMENTS

I would like to acknowledge the capable and cooperative help I received during this work from Dean Thornberg of the antenna manufacturers, dB Systems, Inc., from the staff of Lincoln Laboratory's Antenna Test Range, principally John Magnuson and Bob Burns, from Ed Chateauneuf of Div. 7, from Bart Cardon of Group 41, and from Sylvia Altman, Ed Bayliss, Doug Burgess, Pete Collins, Pete Daly, Ralph Halvorsen, Bill Harman, Arnie Kaminsky, Bob Kenney, George Knittel, John Maccini, John O'Rourke, Richard Potts, and Ken Saunders of Group 42. They are all experts at what they do.

TABLE OF CONTENTS

LIST OF ILLUSTRATIONS

LIST OF ILLUSTRATIONS
(Continued)

LIST OF TABLES

1. INTRODUCTION

GPS-Squitter [1, 2] is a concept in which each aircraft broadcasts its current position at a rate of twice per second using information derived from the Global Positioning System (GPS). The transmissions employ waveforms selected from the current set of internationally standardized Mode S surveillance waveforms. The carrier frequency is 1090 MHz. These broadcast position signals allow other aircraft or ground stations to maintain surveillance of the aircraft using inexpensive antennas and receivers. For the ground stations required for surveillance of en-route aircraft, the proposed system includes a six-sector antenna. Its six azimuthal sectors, each with its separate receiver, together provide the full 360 degrees of azimuthal coverage that a single omnidirectional antenna could provide but with higher gain, and therefore greater range. The separate sectors also limit the number of aircraft being processed by any one receiver, and thereby allow higher total traffic densities to be handled.

The following sections describe, in sequence, the generation of the detailed technical requirements for the antenna, its physical embodiment in the form proposed and built by the chosen contractor (dB Systems Inc., of Salt Lake City), the results of antenna range measurements of its gain patterns, and the results of its operational coverage test.

Three other topics included are, first, some data illustrating the use of the antenna in an emergency role for direction finding, in case GPS-derived position is temporarily lost; second, the application of the antenna in its current location to compiling performance statistics of currently operating aircraft transponders; and third, in an Appendix, the results of a theoretical study of the operating characteristics of the antenna on a buoy-mounted en-route 'ground' station, including the effects on the link of buoy pitching and sea-reflection multipath.

2. THE ANTENNA

2.1 REQUIREMENTS

The gain pattern requirements for each sector of the antenna were developed by a tradeoff among the following four goals:

i) maximizing the minimum signal received from an aircraft anywhere in the coverage sector,

ii) achieving a sharp roll-off at the horizon of the elevation gain pattern to suppress ground-reflection multipath,

iii) minimizing the gain, and hence the fruit, over the azimuthal backlobe region,

iv) creating a simple, rugged, low-cost, pole-mountable unit.

The ideal shape above the horizon of a vertical section through the antenna pattern is determined by the need to deliver to the receiver a constant signal level from an aircraft flying from the horizon towards the ground station at an altitude equal to the maximum aircraft operating altitude. This shape is the classic cosecant-squared pattern, modified by the effect of the earth's curvature. The ideal azimuthal pattern for each sector is constant over its 60-degree coverage area and zero elsewhere.

The specific numerical values for the gain requirements of each sector were generated by trading off these desired pattern shapes with the constraints imposed by the antenna aperture allocated to the sector. To keep the overall physical package consistent with item (iv) of the requirements, this aperture was constrained to be of relatively modest extent in the horizontal direction. The vertical aperture is considerably larger because the pattern directivity and complexity is greater in the vertical direction. In addition, for convenience in handling and mounting, additional length is preferable to additional girth.

The specific gain requirements, extracted from the RFP, are reproduced in Appendix A. Also included there are the requirements concerning weather, mounting, power monitoring, peak power, input impedance and VSWR.

2.2 PHYSICAL DESCRIPTION

Each of the six linear arrays is a modified omnidirectional DME (Distance Measuring Equipment) antenna — a vertical linear array of circumferential slots on a metal cylinder fed by a time-delay equalized RF distribution network. The modification consisted of lengthening it to create a larger gain at the horizon than the standard DME antenna.

The 60-degree azimuthal sector beam was created by mounting a cylindrical reflector, curved in the horizontal direction, behind each linear array. The assembly of all six sectors, before the radome is in place, looks like a six-fluted cylindrical column with a linear slotted feed array running along the focal line of each flute. Figure 1 is a photograph of the antenna on the roof top antenna mount at the Antenna Test Range. Figure 2 is a line drawing showing some of its internal details. The complete radome-enclosed assembly is a cylinder eight feet tall and 23 inches in diameter. It weighs 250 pounds.

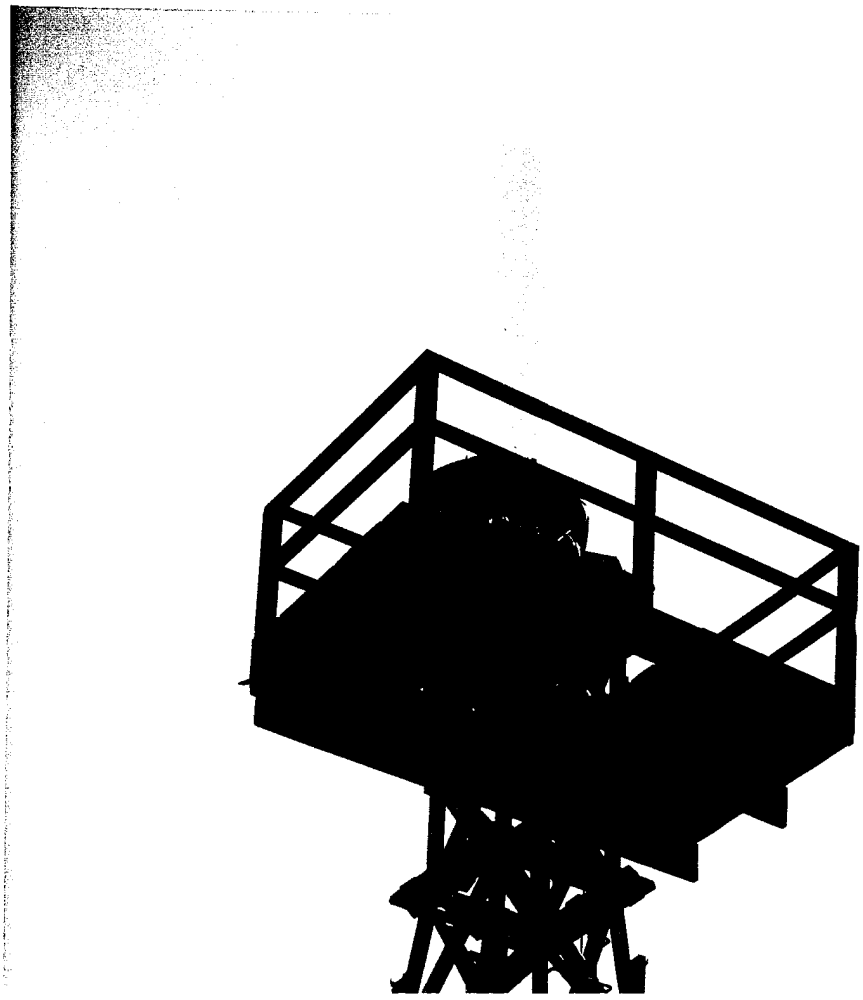

Figure 1. The antenna on a mount on the roof at the Antenna Test Range.

MULTI-SECTOR ANTENNA

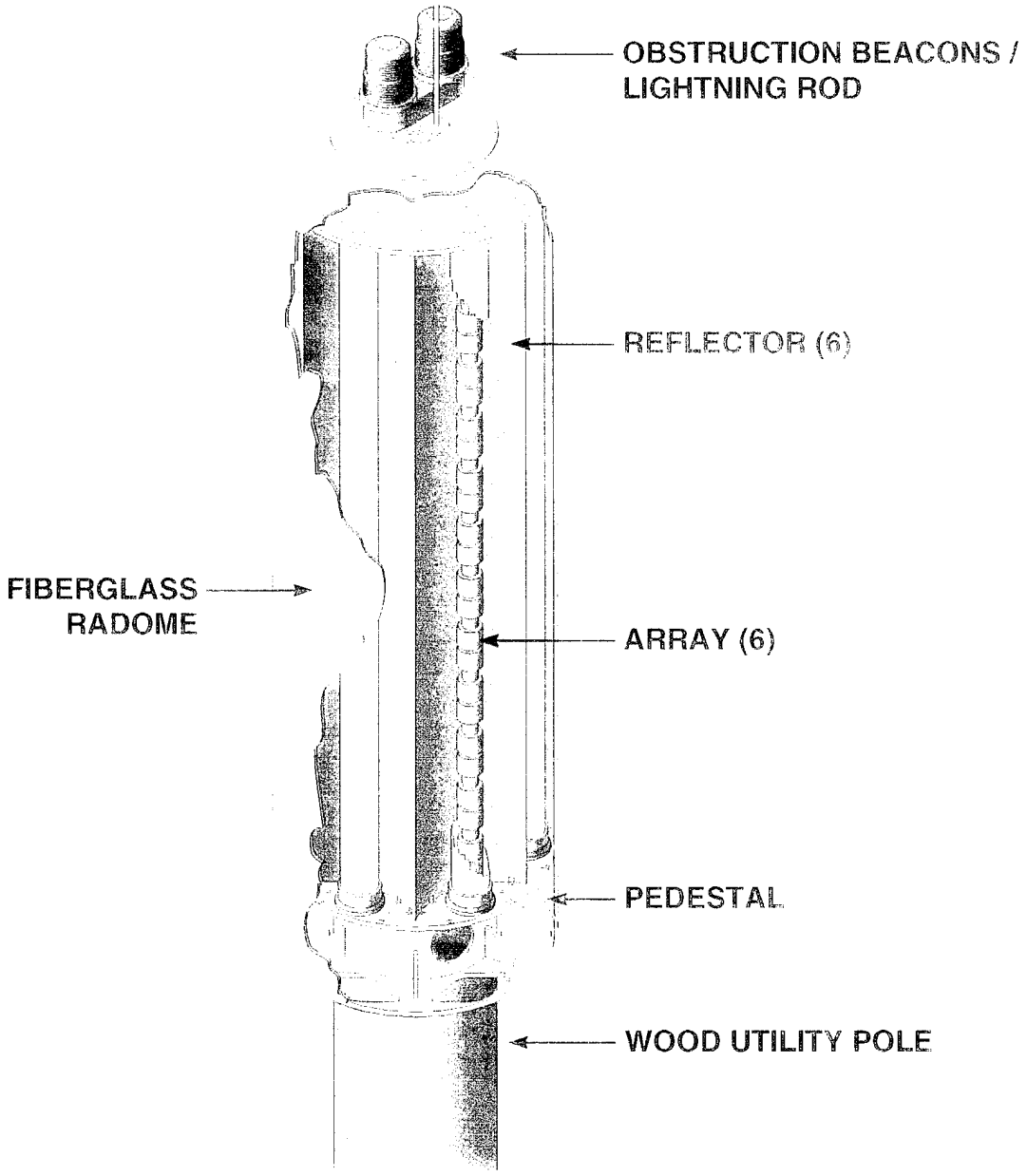

Figure 2. Interior details of the antenna.

2.3 ELECTRICAL PROPERTIES

The gain patterns of the antenna were measured at Lincoln Laboratory's Antenna Test Range, operated by Group 63. Principal-plane patterns, vertical and horizontal, were taken for all six sectors at both 1030 and 1090 MHz. The range was calibrated with a standard gain horn.

The results, shown in Figures 3 through 6, confirm first, that the gain patterns for all six sectors and both measurement frequencies are essentially identical, and second, that to within the probable measurement error, they meet the specifications. The dashed line boxes and angles mark the limits defined by the specifications. The dotted limits on the azimuth graphs denote the bound placed on the average gain over the indicated range of angles. The rapidly changing gain in the azimuth backfire direction is spurious. It is due to reflections off trees and bushes behind the antenna.

2.4 COST

The total cost of the prototype unit was $38,672, including the cost of design and preliminary testing. In production quantities, the unit cost is estimated to be less than $30,000.

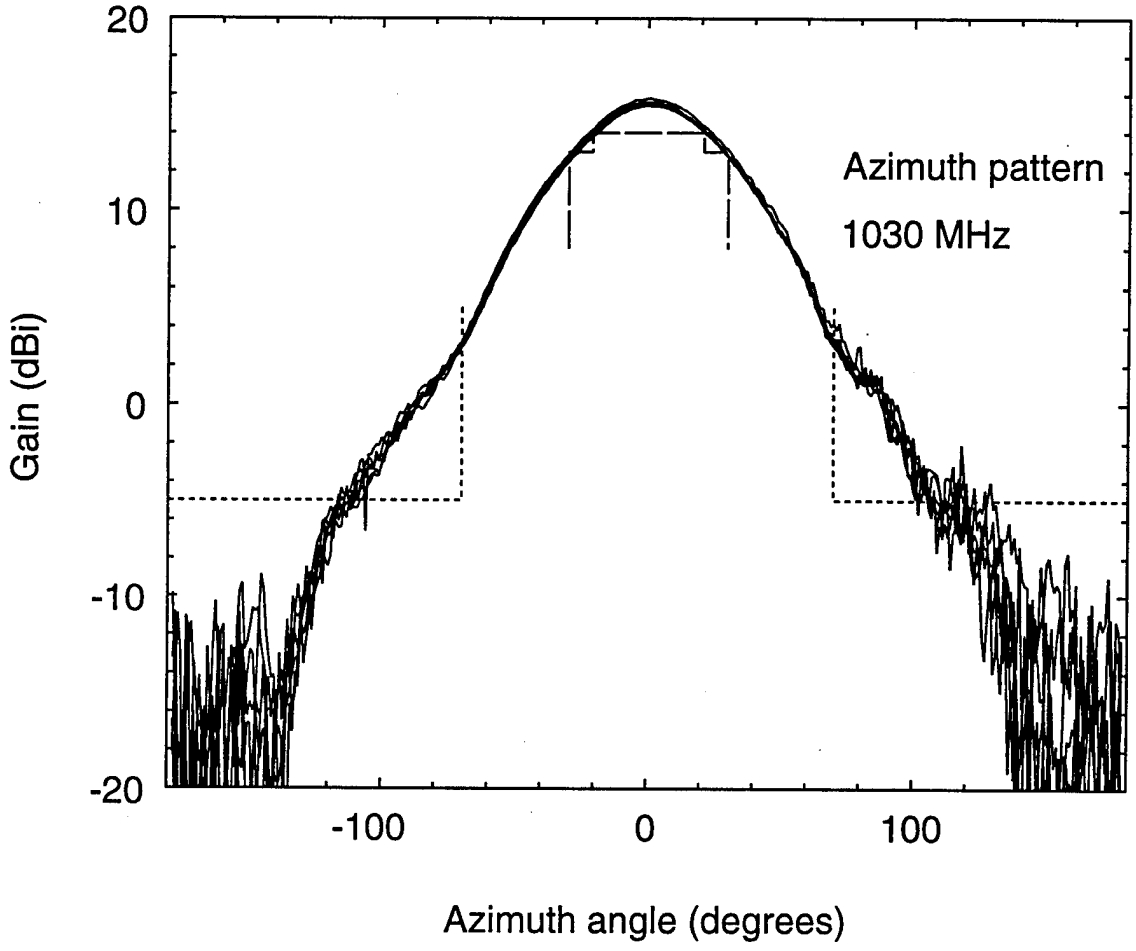

Figure 3. Measured azimuth gain patterns at 1030 MHz for all six sectors, in decibels with respect to an ideal isotropic antenna.

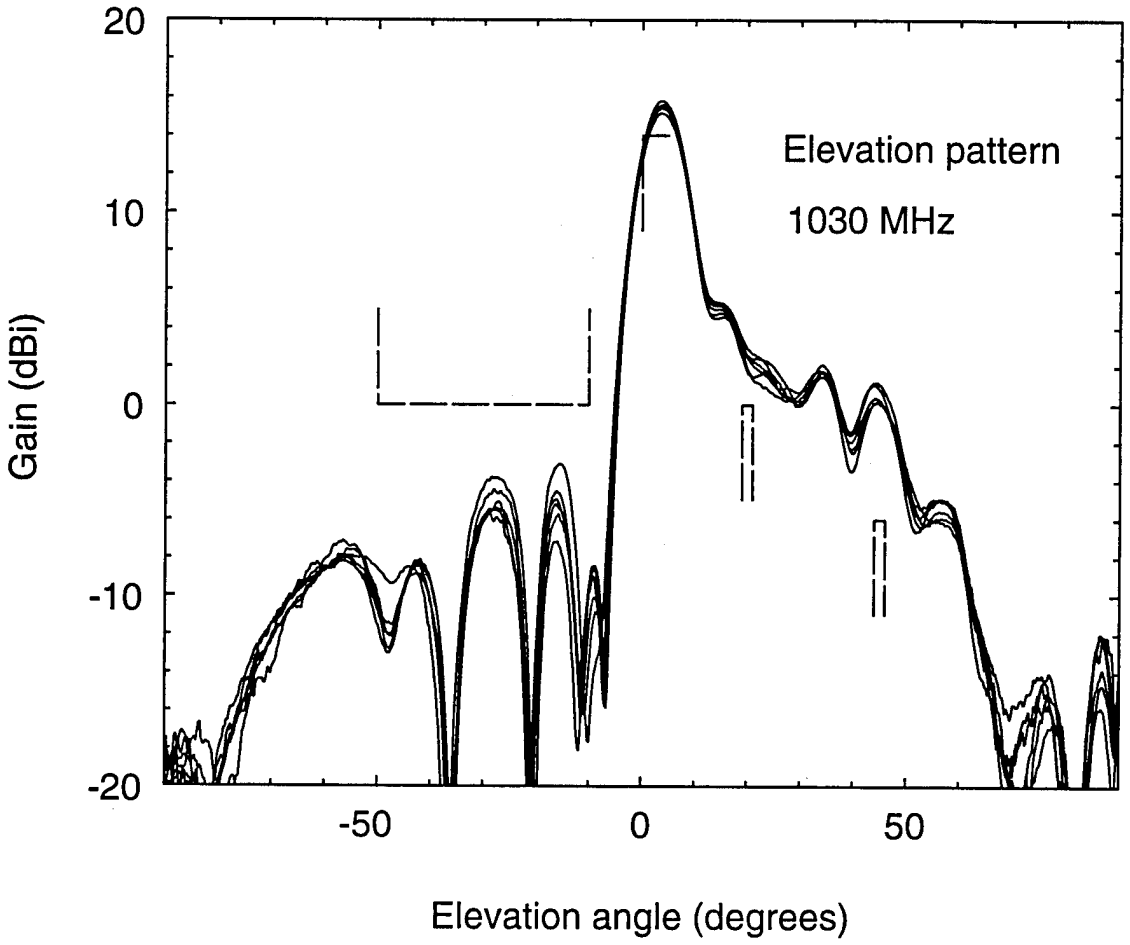

Figure 4. Measured elevation gain patterns at 1030 MHz for all six sectors, in decibels with respect to an ideal isotropic antenna.

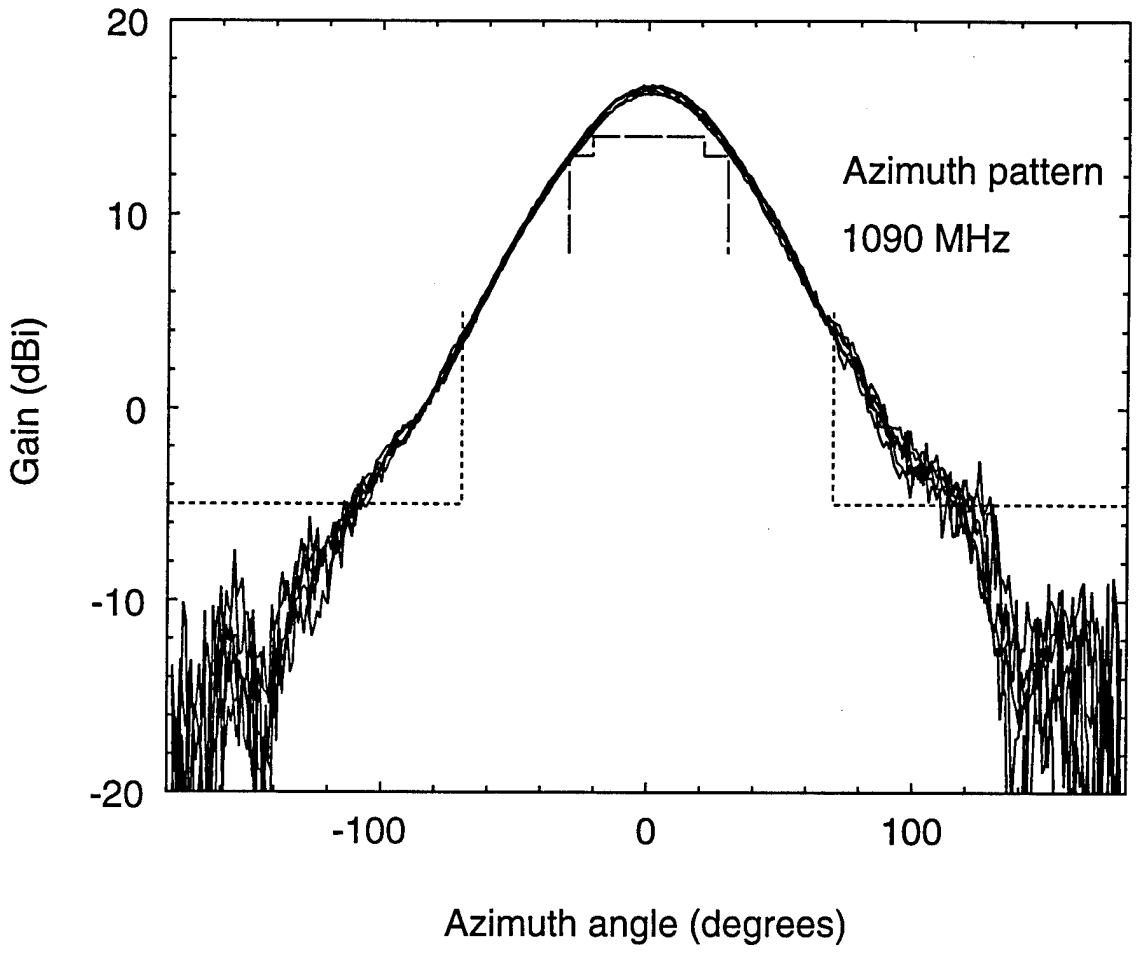

Figure 5. Measured azimuth gain patterns at 1090 MHz for all six sectors, in decibels with respect to an ideal isotropic antenna.

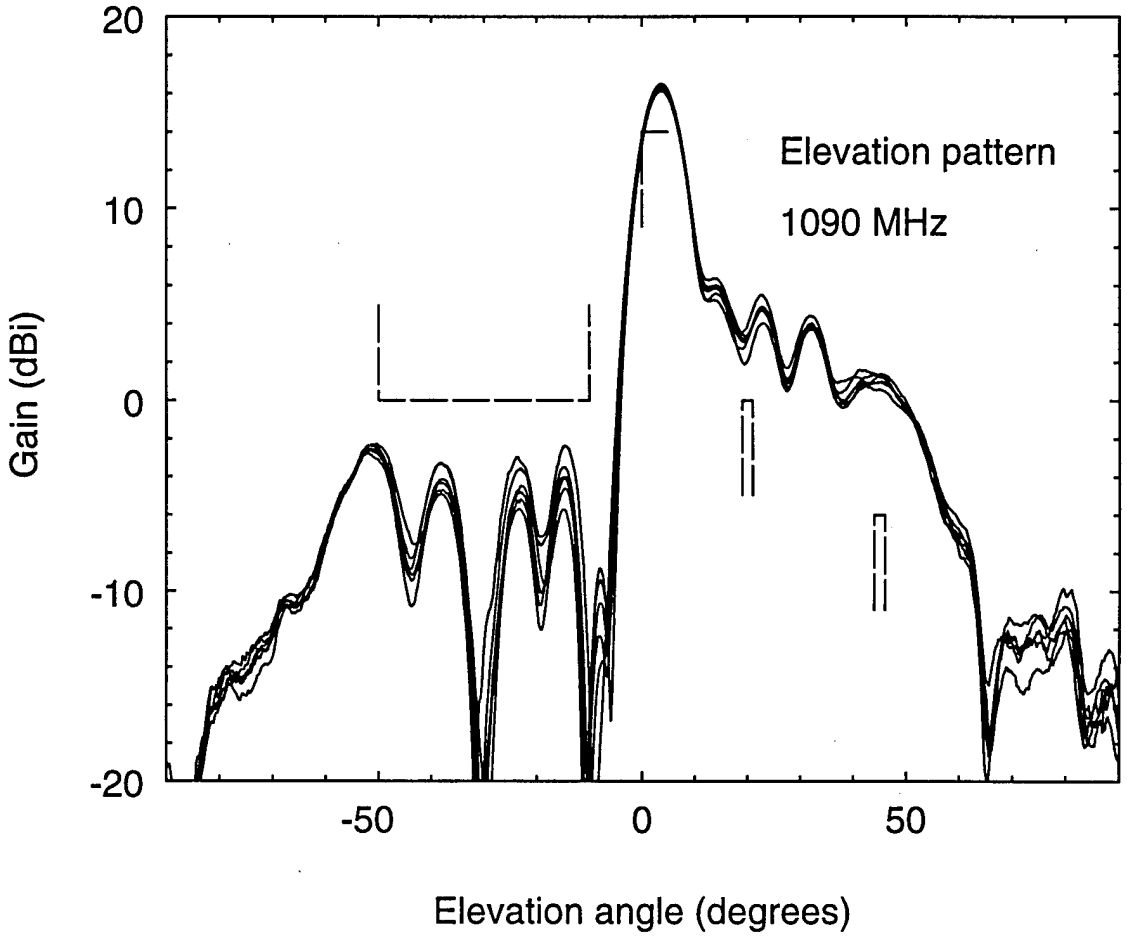

Figure 6. Measured elevation gain patterns at 1090 MHz for all six sectors, in decibels with respect to an ideal isotropic antenna.

3. SYSTEM PERFORMANCE

3.1 COVERAGE

The first system test of the antenna was carried out while the antenna was still in place on the roof top antenna mount at the Antenna Test Range. For the test, short squitters emitted at 1090 MHz from aircraft in the vicinity were collected using one of the antenna's six sector beams connected via an RF preamplifier and an adjustable attenuator to the AMF receiver [3]. At the same time, the Mode S sensor at MODSEF tracked all the aircraft in the area. By matching the IDs of the aircraft tracked by MODSEF with the IDs in the short squitters received via the six-sector antenna, the six sector antenna's coverage area was inferred.

The results of the test are shown in Figure 7. It shows the ground tracks of the aircraft tracked by MODSEF and the sections of those tracks over which short squitters were received by the six-sector antenna.

The duration of the test (about 15 minutes) was not long enough to obtain anything but a sparse sampling of the sector's coverage area. Too few aircraft appeared in the coverage area in that time period to delineate it adequately. However, two conclusions can be drawn. First, the antenna/AMF combination was confirmed to be functioning in that short squitters from many of the aircraft under track by MODSEF were being successfully collected; but second, in some cases squitters were not being received from aircraft that were close enough and in such a direction that one would expect them to get through.

The explanation for this is that at the Antenna Test Range the six-sector antenna was some 1.3 miles from MODSEF, was some 160 feet lower in elevation and was adjacent to a wooded area. Its horizon was therefore typically at a higher elevation angle than that of MODSEF, thereby giving it in some directions a more limited range due to terrain blocking.

To eliminate this uncertainty, the antenna was moved to the 70-foot tall lattice tower adjacent to the MODSEF building. This move placed the antenna laterally within about 200 ft of the MODSEF antenna and at about the same height. Figure 8 is a picture of the antenna being mounted on a 5-foot pedestal on the platform at the top of the tower. In this configuration, both the six-sector antenna and the Mode S sensor were above the tree line and so both had essentially the same distant horizon. In its new location, two sectors of the antenna were connected via tower-top preamplifiers to the two channels of the AMF. (Appendix B includes a description of the data collection equipment.)

The next four figures, Figures 9 through 12, confirm that for aircraft within its sectors of coverage, the six-sector antenna, in combination with the preamplifier and AMF receiver, can receive squitters from everything that MODSEF tracks. That is, in practice its range is limited by horizon cut off rather than by insufficient sensitivity. This performance is consistent with the proposed link budget for the en-route ground station equipped with a six sector antenna, presented in Appendix C.

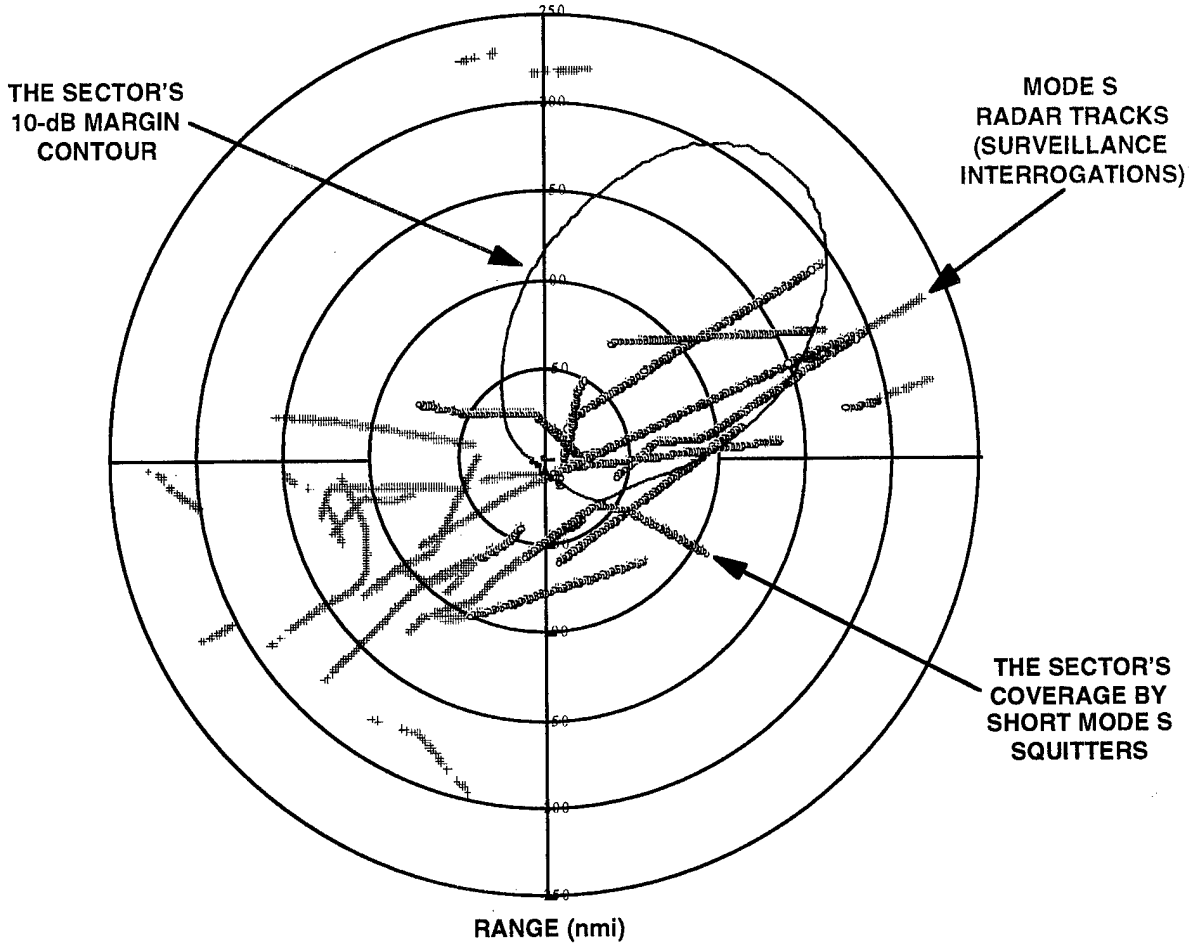

Figure 7. The ground tracks of several aircraft monitored from the Antenna Test Range by a single sector of the six-sector antenna and simultaneously tracked by the MODSEF Mode S sensor. The parts of the tracks over which short squitters were received by the six-sector antenna are shown in black. Where short squitters were not received, the track is blue. The red curve is a polar plot of the sector's aximuth gain pattern. The antenna was located approximately 1.3 miles from MODSEF and lower in altitude by some 160 feet.

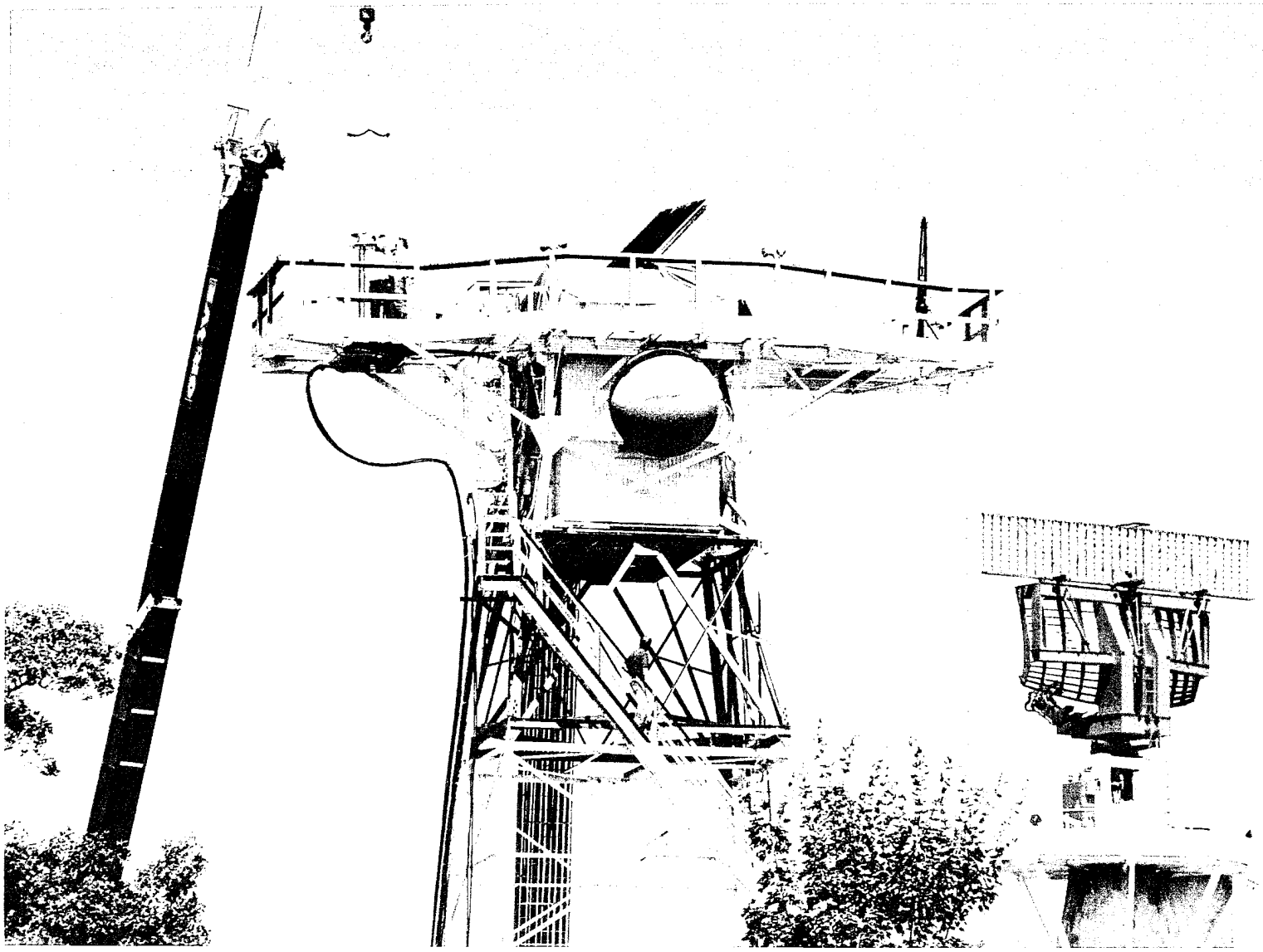

Figure 8. The antenna being mounted on the 70-foot lattice tower adjacent to the MODSEF Mode S Sensor.

AIRCRAFT POSITIONS IN TIME INTERVAL 54940 TO 56620 SECONDS ON 95.317
SOURCE: AMF RECORDED SQUITTERS (AT 07 db)
(POSITION DATA RECORDED AT MODSEF)

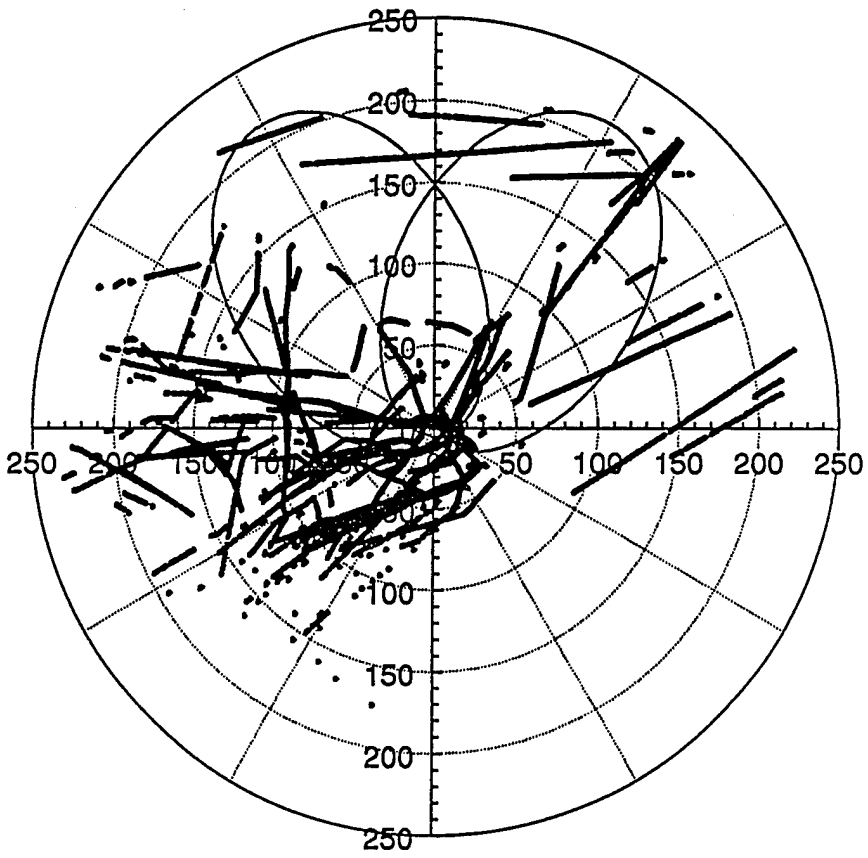

RANGE IN NAUTICAL MILES

Figure 9. The ground tracks of short squitters collected by two sectors of the six sector antenna mounted on the lattice tower. The source location of each squitter was determined by interpolating MODSEF tracking data for the originating aircraft. The gain patterns of the two antenna sectors, expressing the range at each azimuth for which the signal margin is 10 dB, are also shown.

AIRCRAFT POSITIONS IN TIME INTERVAL 54940 TO 56620 SECONDS
SOURCE: MODSEF DATA COLLECTION 95.317
(FOR 7 db SETTING)

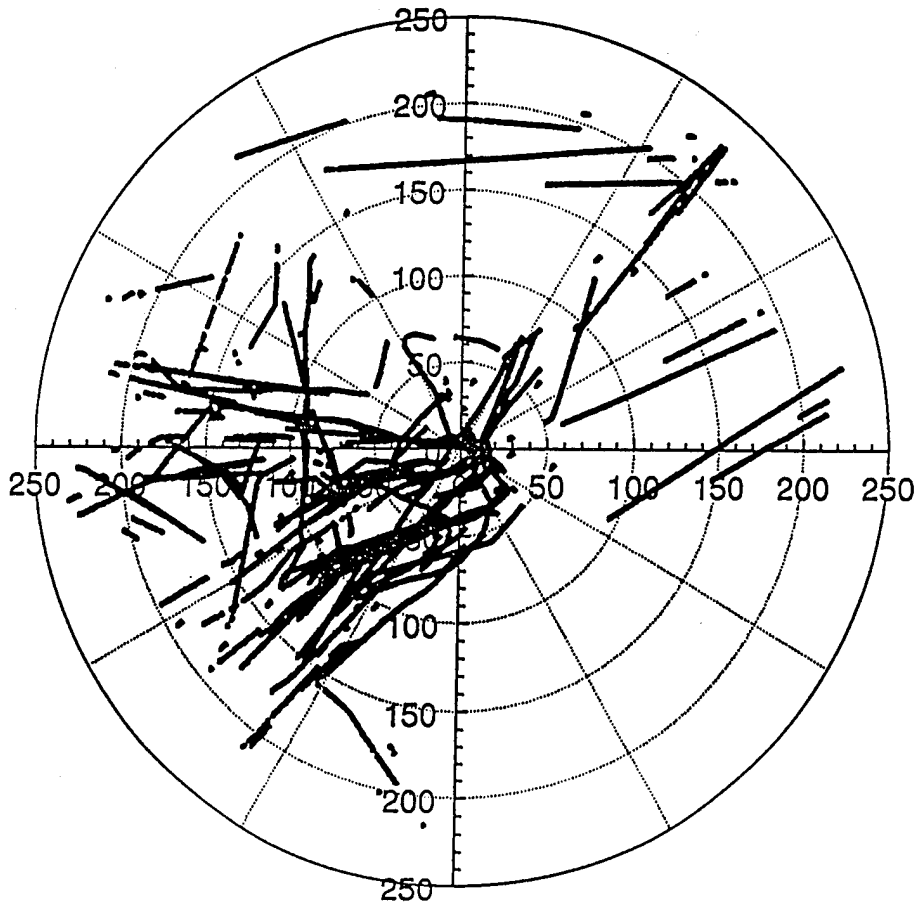

RANGE IN NAUTICAL MILES

Figure 10. The ground tracks of all the aircraft tracked by MODSEF during the time period covered by the previous figure.

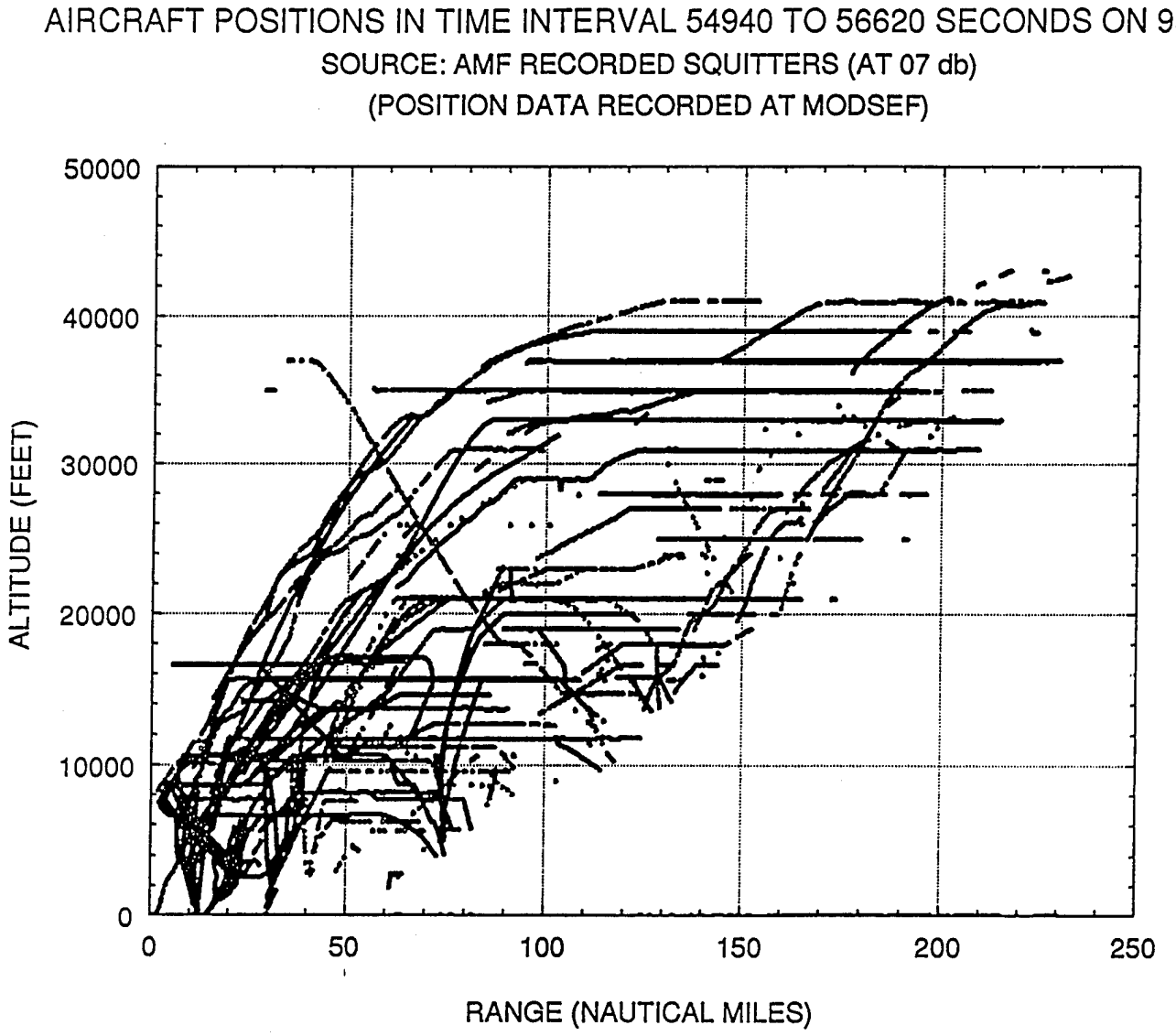

Figure 11. The altitude tracks of short squitters collected by two sectors of the six sector antenna mounted on the lattice tower. The source locations of each squitter was determined by interpolating MODSEF tracking data for the originating aircraft.

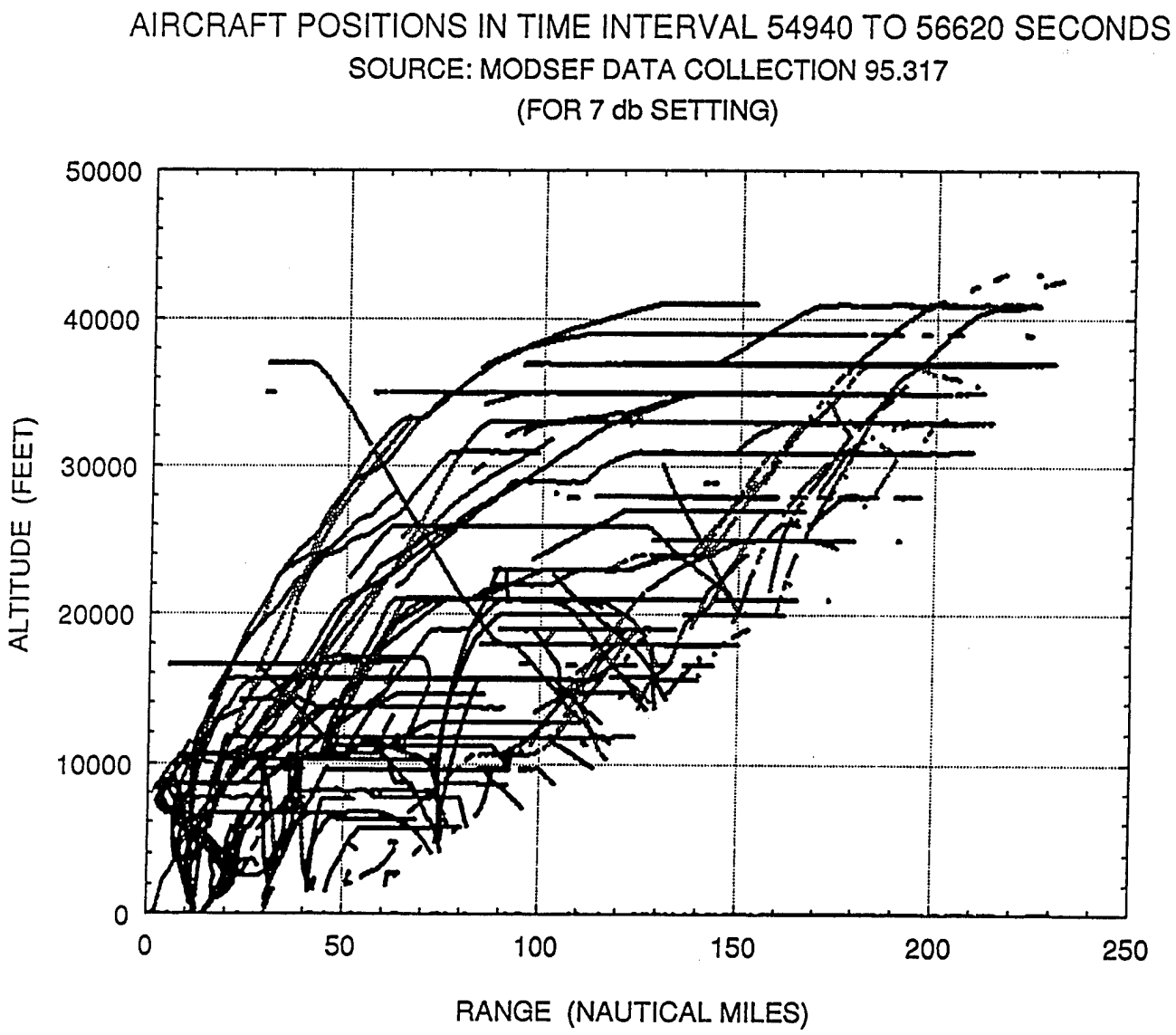

Figure 12. The altitude tracks of all aircraft tracked by MODSEF during the time period covered by the previous figure.

3.2 SURVEILLANCE RELIABILITY

An important requirement of GPS-Squitter surveillance is the steady reception of the squitters broadcast from each aircraft. Figures 13 through 15 show some data important for assessing this aspect of surveillance reliability that have been collected by the antenna/AMF combination.

Figure 13 is a plot of the amplitude of the squitters received from a particular aircraft by the two active sectors of the antenna. The aircraft approached the antenna at an altitude of 35,000 ft following approximately the radial at 45-degree true bearing. Squitter reception began at a range of 233 nmi. Because the 4/3 earth's radius refraction model predicts that an aircraft at this height first breaks horizon when its range is 230 nmi, it appears that the start of reception coincided with the first emergence of the aircraft above the horizon. By comparison, MODSEF's first tracking report on the aircraft did not occur until the aircraft was 20 nmi closer in range.

1) They were received steadily.

2) Their amplitude, apart from some scintillation as the propagation path first cleared the horizon, steadily increased as the range decreased, indicating that there existed only a weak multipath component reflected from the tree tops that formed the ground plane.

3) There was a clear amplitude bifurcation of the squitter amplitudes in both sectors, reflecting the standard procedure of alternately emitting the squitters through the top and bottom antennas on the aircraft.

4) The squitter amplitudes in Sector 1 were some 17 dB less than those in Sector 2. This would be expected, because the aircraft bearing implies, from the measured antenna patterns shown in Figure 5, a pattern gain difference of about 13 dB, and the Sector 2 receiver was overall 3.5 dB more sensitive than that of Sector 1. (The calibration data in Appendix B imply that the squitter powers in dBm at the output ports of the two active antenna Sectors 1 and 2 are to be evaluated by subtracting respectively 119.7 and 123.2 from the A/D counts registered by their receivers.)

An expanded portion of this figure, clearly illustrating alternating squitter transmissions between the top and bottom aircraft antennas, is presented as Figure 14. Since the gain of the top antenna in any given direction is different in general from that of the bottom antenna, but the transmitted power is essentially the same, the received power cycles back and forth by an amount equal to the gain difference.

Figure 15 presents the squitter-reception data in another way. It shows the cumulative received squitter count as a function of time for three different aircraft. Two are Canadian aircraft traveling across the field of view and one a German aircraft (the same one from which the squitters plotted in Figures 13 and 14 were transmitted) traveling radially. If the squitters had been transmitted strictly at a rate of one per second and if every squitter had been successfully received by the receivers, then these cumulative squitter count curves would be straight lines with a slope of unity.

The curves for the Canadian aircraft are approximately straight with a slope of 0.76 squitters per second, suggesting that the squitters were received steadily with an average success rate of more than 75 percent. The rate at which squitters were received from the German aircraft was less, initially, than that from the Canadian aircraft, no doubt because of its low elevation angle

and greater range, but in the later stages of the coverage shown in Figure 15, the rate for all three was about the same. The reason that the average success rate is not closer to 100 percent has not been determined. Figure 14 implies that, over the short time interval included in the graph, the success rate was precisely 100 percent. Whether it is because the squitters are being emitted at an average rate of less than one per second, or because system noise or interference are capturing the receiver, remains to be seen.

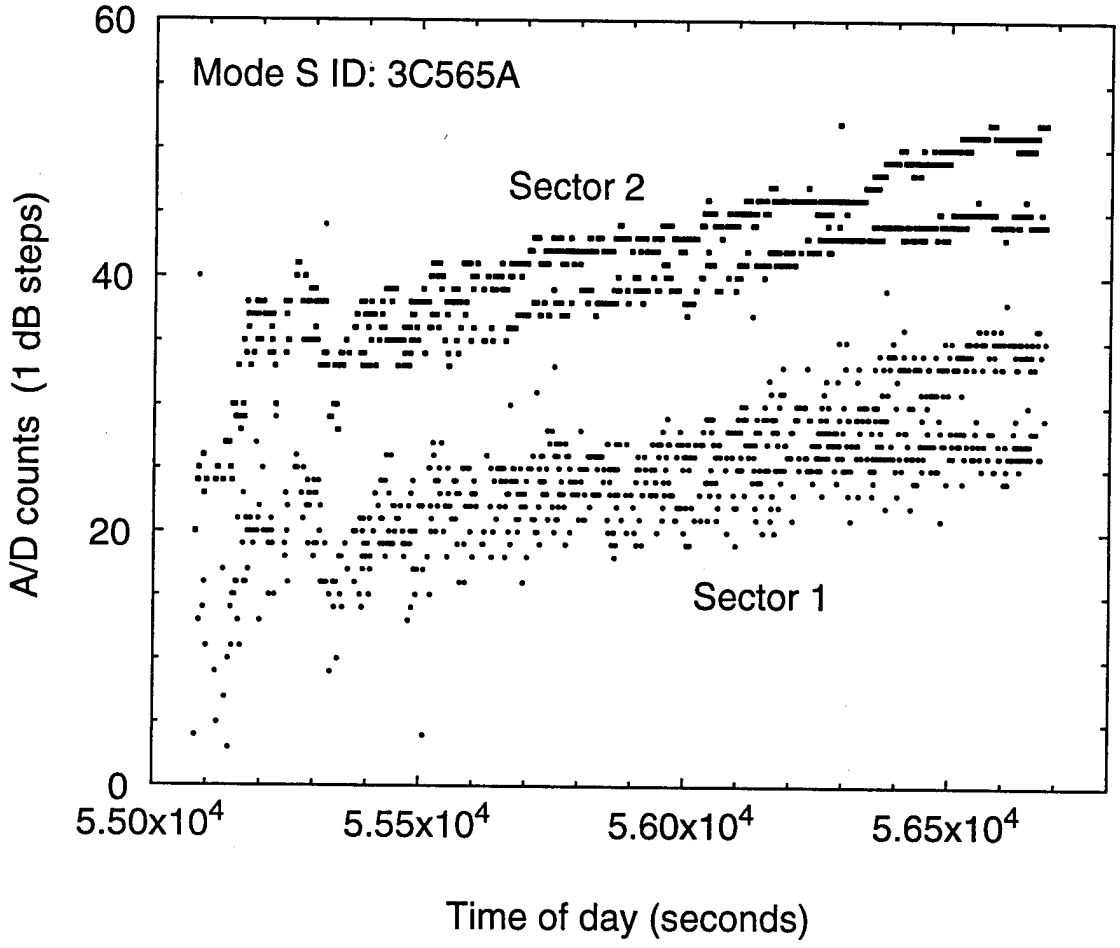

Figure 13. The relative power level of short squitters from a single aircraft received by the two sectors of the six-sector antenna. The aircraft, flying at an altitude of 35,000 ft, first appeared over the north east horizon at a range of 233 nmi. Evident in the data from both sectors is the cycling of the power level as a result of alternating squitter transmissions between the top and bottom aircraft antennas.

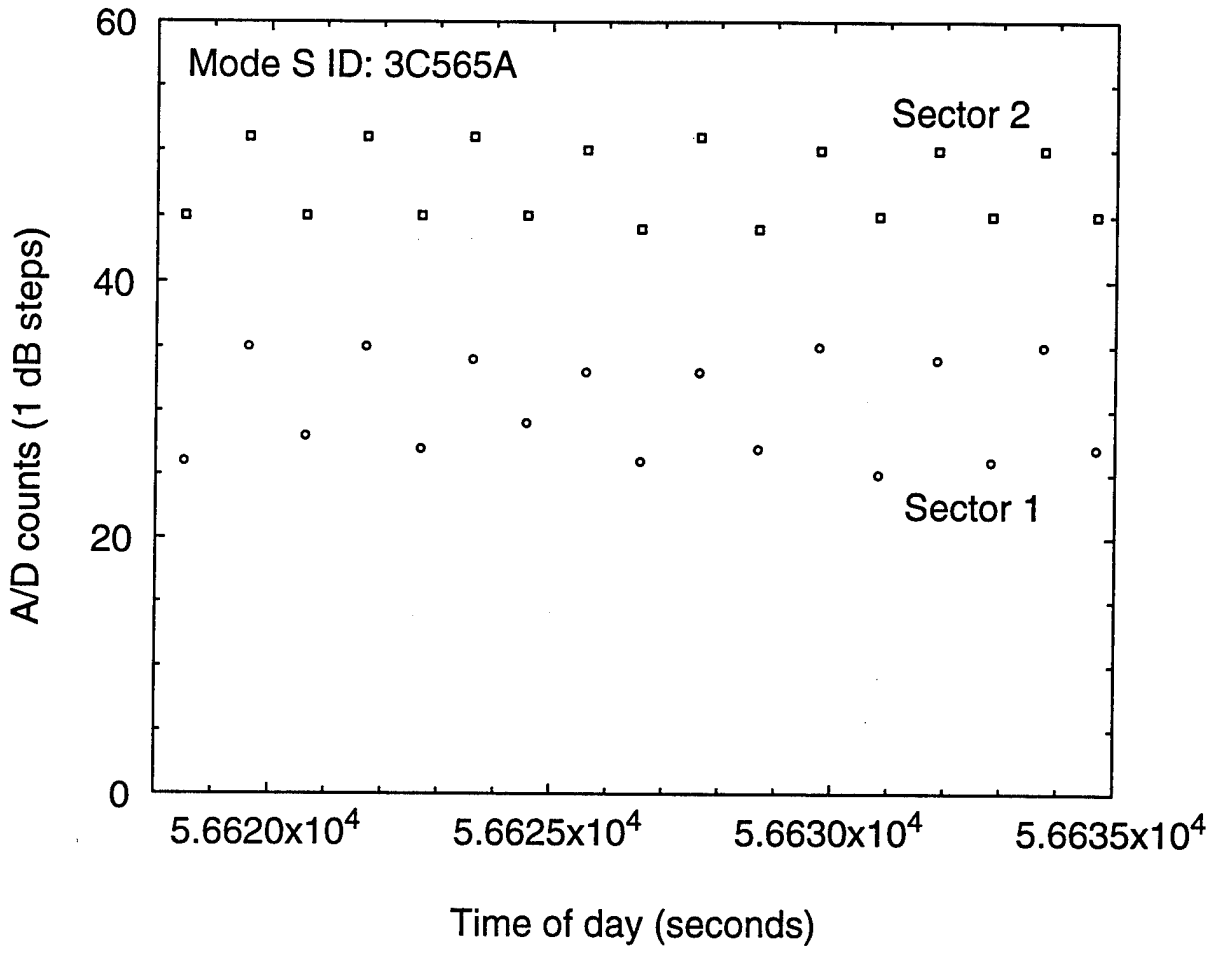

Figure 14. A time expansion of a piece of the previous graph (Figure 13) clearly illustrating alternating squitter transmissions between the top and bottom aircraft antennas.

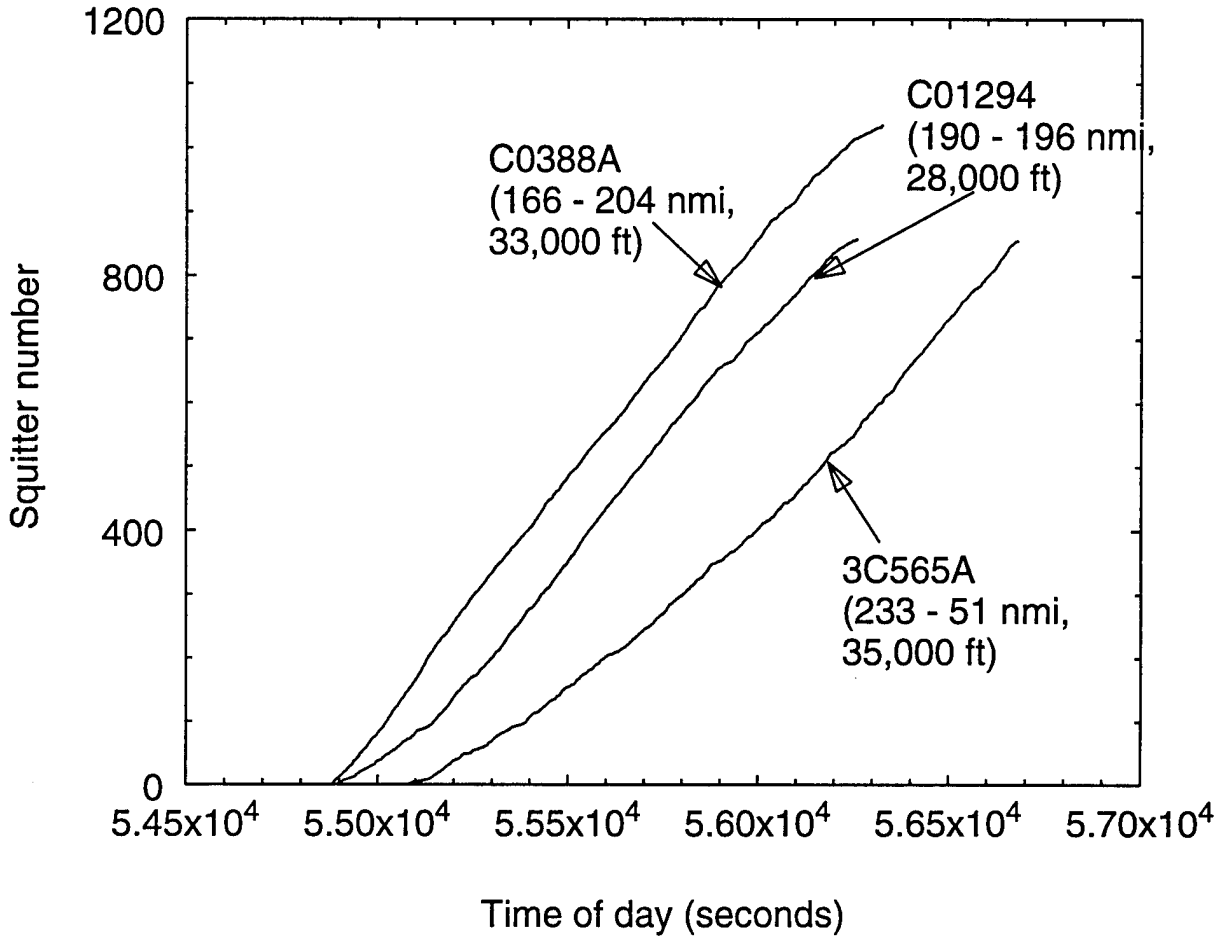

Figure 15. The cumulative count versus time of the short squitters received from three different aircraft by the two sectors of the six-sector antenna.

3.3 DIRECTION FINDING

The main purpose of the multiple beams of the en-route ground station antenna is to provide the station with a greater surveillance range than a single-beam omnidirectional antenna could provide. However, a potential additional benefit the separate beams offer is the opportunity to measure the bearing of the squittering aircraft. This may be useful as an emergency surveillance back-up function in case GPS-derived position information is temporarily lost.

The squitters collected from the two Canadian aircraft allowed this function to be investigated. First, one of the aircraft was used to derive a direction finding calibration curve, defining the azimuth offset of the target aircraft as a function of the difference in the power received by the two channels for each squitter. Then the power levels in the two channels of the squitters received from the other Canadian aircraft were used to demonstrate the use of this calibration curve to measure target azimuth. The results are displayed in Figures 16 through 18.

The calibration curve shown in Figure 16 is a third degree polynomial fitted to the power difference data. The rms variation of the power differences from this curve implies that if this curve had been used to estimate the bearing of the target aircraft from these power differences, the rms error would have been 3.2 degrees. In a more realistic test, when the curve is applied to the power differences of the squitters received from the other Canadian aircraft, as in Figure 17, the rms error is 4.2 degrees. However, if 7-point smoothing is applied to the power differences before using the calibration curve to infer bearing, the rms error reduces to 1.9 degrees.

This demonstration of direction finding, involving only the one target aircraft at a large range and low elevation angle, can be regarded only as a preliminary result proving feasibility. Further investigation over a wider range of operating parameters is necessary before a full assessment can be made.

These results promise an accuracy of the antenna for power-difference direction-finding of about 2 degrees. A more elaborate, and potentially more accurate, way of direction finding would be to combine the sector output voltages coherently at RF, as in a monopulse antenna. This method was not included in the present investigation because it would require a more complicated receiver.

It should be noted that the horizontal blank band running through the power level data in these last three figures, Figures 16 through 18, is due to a stuck bit in the AMF A/D converter and not to missed squitter receptions. Power level values falling in this band were assigned by the A/D converter to values lying immediately above or below the empty band. The vertical blank bands also were not caused by missed squitters. They are due to missing tracking reports from MODSEF. If the time period for which reports are missing is too great for the interpolation algorithm to accept, no tracking data are assigned to the squitters. In particular, no bearing information is generated for the affected squitters, and so they do not appear on the three figures.

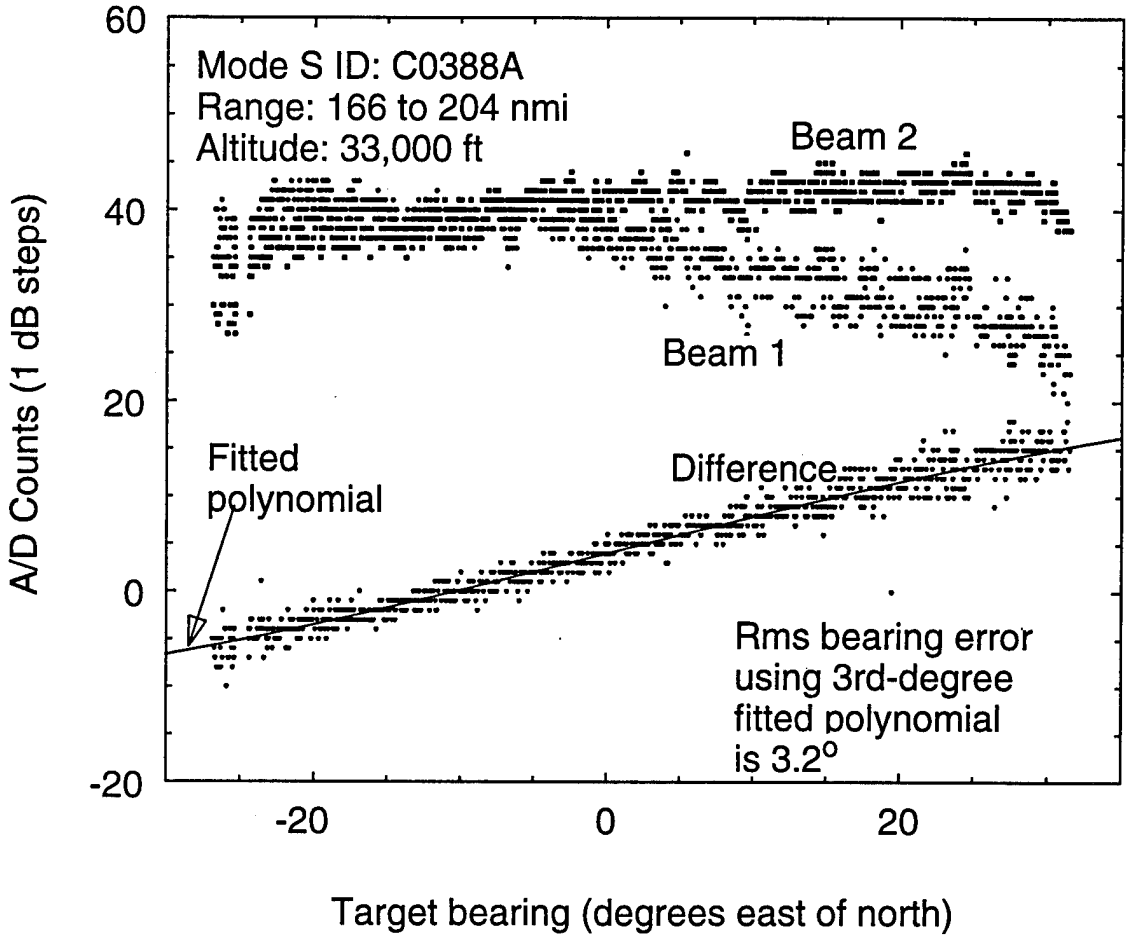

Figure 16. The power level of squitters received by the two sectors from an aircraft moving across the antenna's field of view and a third degree polynomial fitted to the power level differences between the two sectors. This establishes the calibration curve for direction finding.

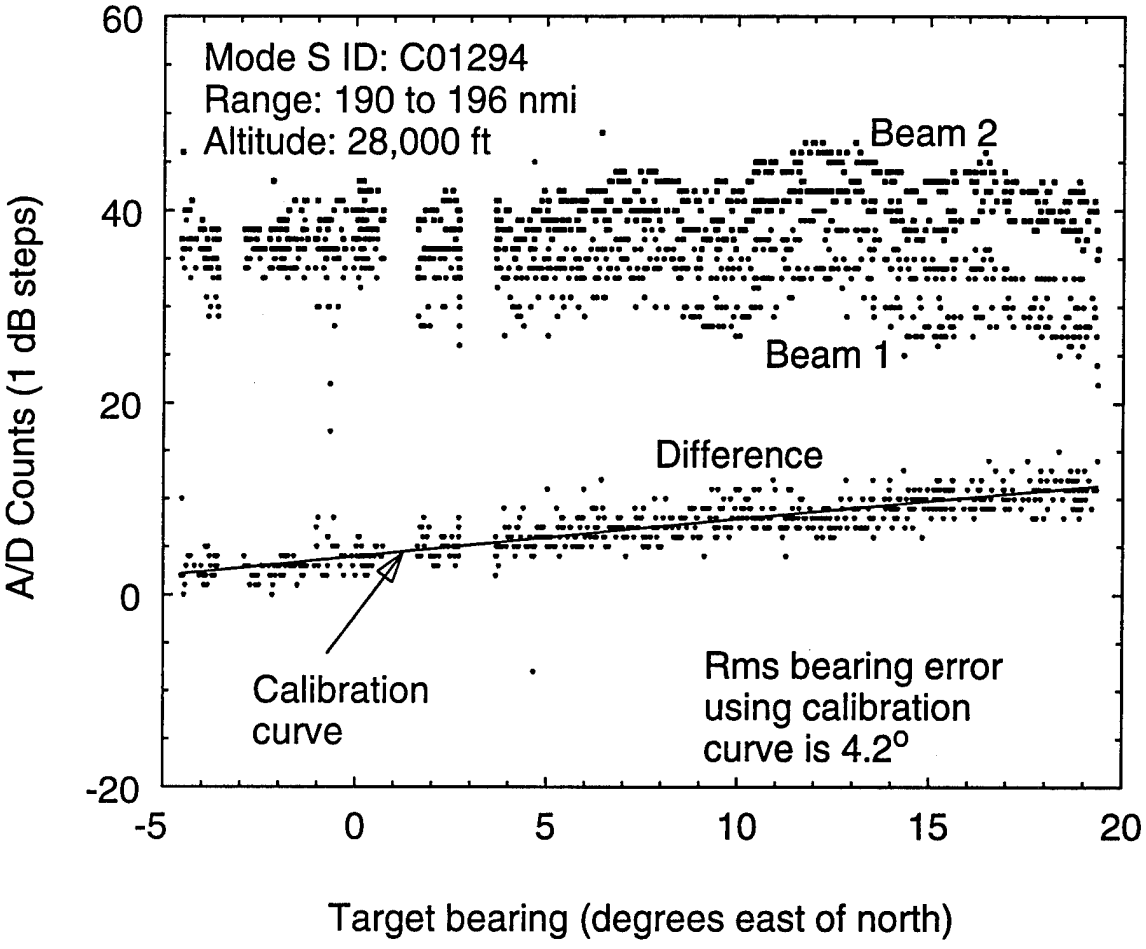

Figure 17. The power level of squitters received by the two sectors from a different aircraft from that used to define the calibration curve of Figure 16 and the new set of power level differences between the two sectors compared with the calibration curve.

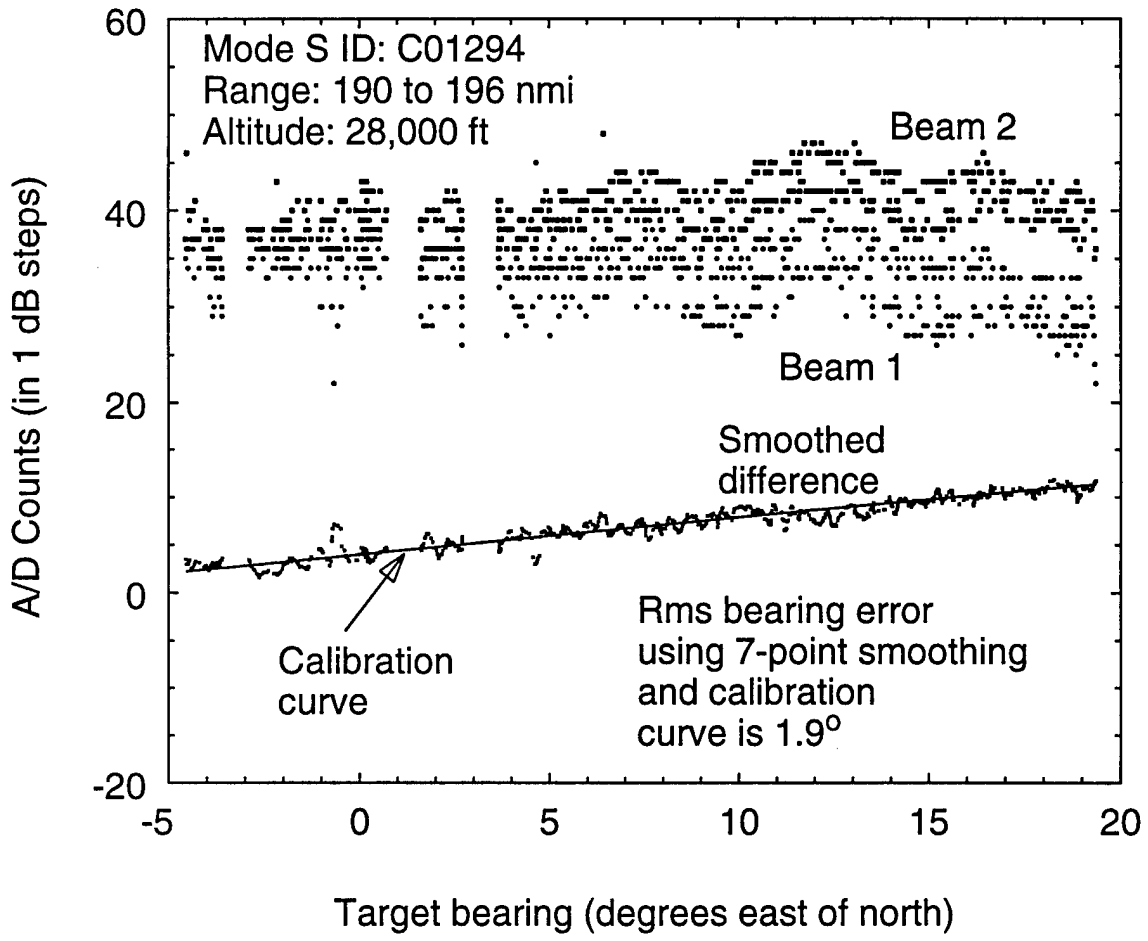

Figure 18. The same as Figure 17 except that a 7-point smoothing operation has been applied to the power level differences.

4. SURVEY OF TRANSPONDER ERP DISTRIBUTION

The six-sector antenna in its current location is well placed for surveying the operating characteristics of the many transponders currently carried on aircraft using New England's airspace. Figures 19 and 20 are examples. They present statistics of transponder effective radiated powers (ERP).

The first one shows the histogram of the ERPs of all 3375 squitters received during a five hour period that originated on aircraft within the range limits 45 to 50 nmi of the 60-degree azimuth sector covered by Sector 2. The ERPs were calculated from the measured received power by applying the proper correction factors to account for the range and for the shape of the antenna gain pattern, in azimuth and elevation. The evaluation of the elevation angle was adjusted, using the usual 4/3 earth radius approximation, to account for the main refractive effect of the atmosphere. The relevant formulas are listed in Appendix B.

As expected, the ERPs are distributed widely about the nominal value of 54 dBm. This is because the transponders themselves differ in their power output and especially because the gain of the transmitting antennas on the aircraft varies strongly with elevation angle and also with azimuth angle. The fact that a few very low ERPs were measured is not necessarily an indication that the transmitted power on some aircraft is below the minimum required level (48.5 dBm for low altitude, slower aircraft and 51 dBm for others). To overcome the problem that the propagation path from a single aircraft transmitting antenna will sometimes be blocked by the body of the aircraft, most aircraft are equipped with two antennas, one on the top of the fuselage and one on the bottom. The short squitters are then transmitted alternately through the two antennas, ensuring that when one squitter is blocked the next one will get through. Many of the low ERPs appearing in Figure 19 are therefore likely to have emanated from the partially blocked member of a pair of aircraft antennas.

A better indication of the state of the surveillance system could be obtained from the squitter data plotted in Figure 19 by discarding all those squitters that emanated from the more disadvantaged member of each antenna pair. The problem here is the difficulty of identifying these squitters. The squitters are not emitted at a steady one-per-second rate, occasionally a squitter is not received due to garble, and the identity of the more disadvantaged member of an antenna pair switches from one antenna to the other as the aircraft's aspect angle varies. An approximate procedure, suggested by Bill Harman of Lincoln Laboratory, that approximately accomplishes the required editing is that of retaining, for each aircraft, the squitter with the maximum ERP received in successive contiguous 10 s time windows, and discarding the rest. An additional criterion, added to prevent spurious inclusions at the time, range, and azimuth boundaries of the coverage volume, is that the maximum for each aircraft in each 10 s window is retained only if at least three squitters were received from the aircraft in that window.

This editing procedure reduced to 355 the number of squitters in the data base. Their distribution, shown in Figure 20, is seen to conform very well with the requirements, which specify lower and upper limits of the transmitted transponder power of 48.5 and 57 dBm. That the range of the ERPs plotted in the figure exceeds this by a few decibels is accounted for by variations of the transmit antenna gain from the nominal 0 dBi.

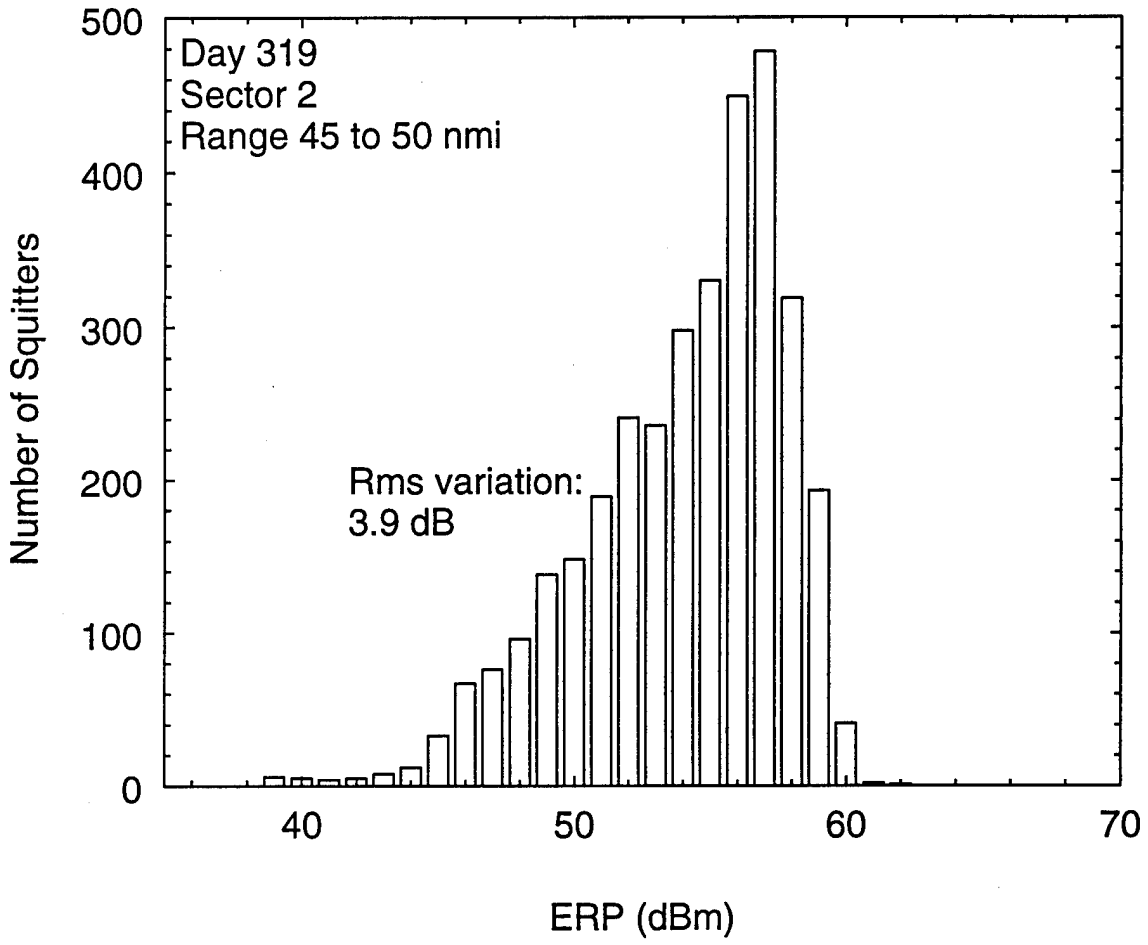

Figure 19. The distribution of the ERP of all the short squitters received over a given time and range interval from aircraft in the 60-degree coverage sector of Sector 2.

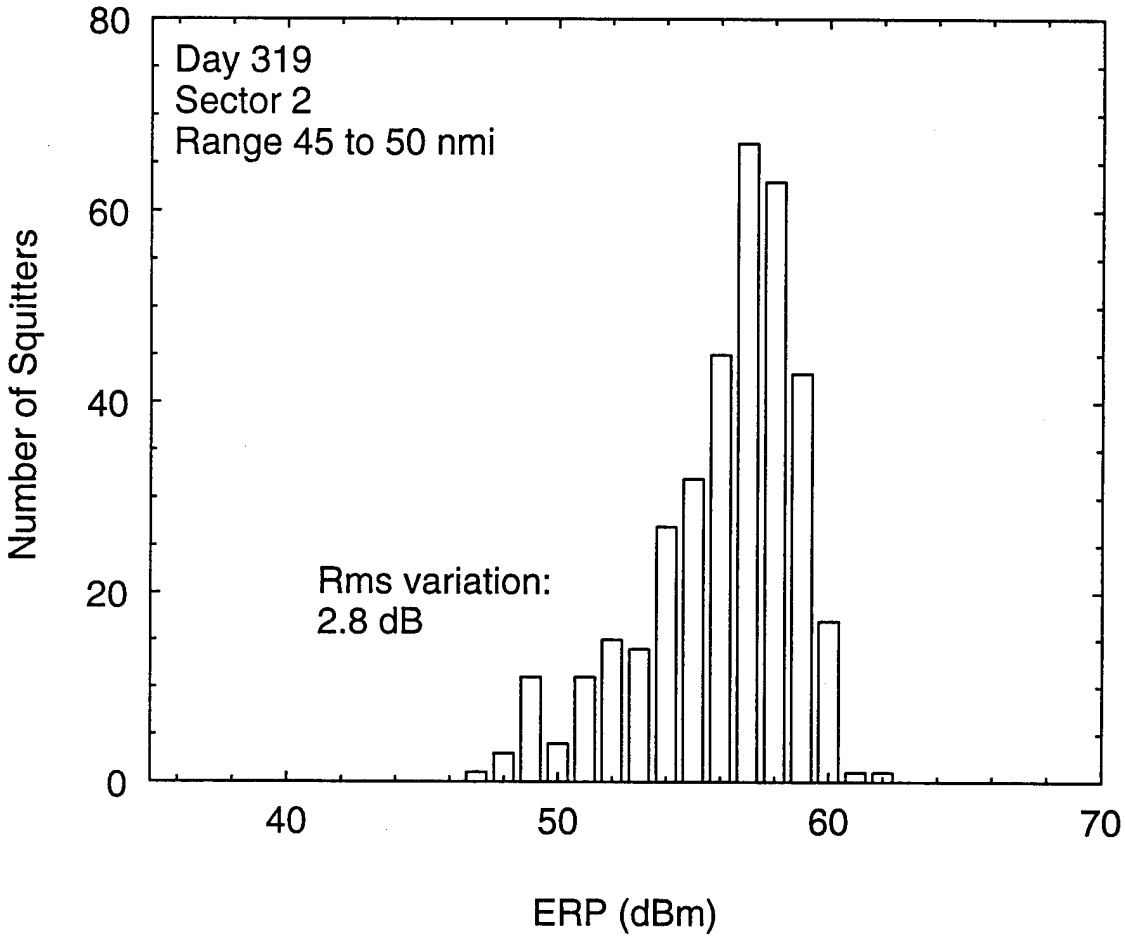

Figure 20. The distribution of the maximum ERP received from each aircraft in successive 10 s time windows for all the short squitter received over a given time and range interval from aicraft in the 60-degree coverage sector of Sector 2.

5. CONCLUSIONS

Antenna-range measurements on a six-sector antenna built for a pole-mounted GPS-Squitter en-route ground station verified that it meets its design goals. Reception tests in which the antenna was used to collect short squitters broadcast by air traffic being tracked by the MODSEF Mode S sensor, demonstrated its system performance. Together, its six uniformly spaced, contiguous 60-degree sectors cover the complete 360 degrees of azimuth at the two Mode S frequencies, 1030 and 1090 MHz. When equipped with its receivers, the antenna achieves a maximum operational squitter reception range in excess of 200 nmi. These results confirm that the antenna is ready for integration and test in a complete en-route ground station.

Additional investigations demonstrated the potential application of the antenna for direction finding in case GPS-derived position is temporarily lost; confirmed its usefulness when paired with MODSEF for surveying the statistics of aircraft transponders' operating characteristics; and developed software for evaluating the use of the antenna on a buoy-mounted en-route 'ground' station, including the effects on the link of buoy motion and sea-reflection multipath.

APPENDIX A: ANTENNA REQUIREMENTS

The antenna requirements, as expressed in the RFP, are as follows:

- the antenna is a multiple beam antenna with six nominally identical sector beams spaced uniformly in azimuth
- each beam covers its separate 60-degree sector of the full circle
- each beam has its own separate input connector
- each beam also has its own separate power monitor connector at which a small fraction of the input power appears
- the antenna mounting is by bolted base flange
- the antenna will not be impaired physically, and it will continue to function electrically, despite continuous exposure to the weather in any part of the United States
- under conditions of severe icing, gain loss of as much as 1 dB in any direction within the 60° coverage sector is acceptable
- there will be no radome unless it is specified in the potential vendor's proposal, and in that case it would be considered to be a part of the antenna system being proposed
- the operating frequency range shall be from 1025 to 1035 MHz and from 1085 to 1095 MHz
- vertical polarization

The gain specifications for each beam are expressed as gain limits applied to the two principal-plane pattern cuts. Elevation angle is defined to mean angle above the horizontal. The horizon is at 0-degree elevation; the zenith at 90 degrees.

For the elevation pattern, taken at the azimuthal centerline of the beam:

- gain no greater than 0 dBi between the elevation angles -50 degrees and -10 degrees
- gain no less than 14 dBi at the horizon
- gain slope no less than 1 dB per degree at the horizon
- peak gain lying between the elevation angles of 2.5 degrees and 4.5 degrees
- gain no less than -0 dBi for the elevation angle of 20 degrees
- gain no less than -6 dBi for the elevation angle of 45 degrees
- no deep gain nulls between the elevation angles of 10 degrees and 55 degrees

And for the azimuth pattern, taken through the peak of the elevation pattern:

- gain no less than 13 dBi throughout the 60-degree sector, including its edges
- gain no less than 14 dBi over at least 70 percent of the 60-degree sector
- mean gain no greater than -5 dBi (-10 dBi preferred) throughout the azimuthal region defined as the set of all points on the complete circle lying further than 70 degrees, plus or minus, from the azimuthal center point of the beam

The remaining specifications for each beam are:

- 2 kW peak power with duty factor no greater than 2 percent
- type N connector for main feed and for power monitor output
- 50 ohm impedance
- VSWR no greater than 2:1

APPENDIX B: DATA COLLECTION PARTICULARS

A block diagram of the data collection equipment is presented in Figure 21. The quantitative particulars are shown in Table 1.

Table 1. Calibration Particulars

	Sector 1	Sector 2
Bearing of Boresight (deg.)	- 30	30
Preamp. gain (dB)	27.9	29.4
Cable loss (dB)	10.2	10.2
AMF calibration (counts - dBm)	102	104
AMF signal threshold (dBm)	- 80	- 80
Sig. thresh. at ant. ports (dBm)	- 87.7	- 89.2

The preamplifier gain is the total gain measured between the antenna output port and the output port of the tower-top preamplifier box. It therefore includes the effect of the loss through the limiter and all the short tower-top connecting cables. The cable loss is the total loss between the preamplifier box output port and the input port to the AMF, but excluding the loss through the two 10 dB attenuators.

The ERP at the aircraft of a received squitter of power P dBm at the frequency 1090 MHz is given by

$$ERP = P + 20 \log (84{,}600\ r) - G\ (\theta, \phi)\ \text{dBm},$$

where r is the range of the aircraft in nmi and G is the antenna gain in dBi as a function of the elevation angle θ and the azimuth angle ϕ from boresight, both angles in degrees. This formula is simply a restatement of the basic link equation expressing the received power as the transmitted ERP plus the receiver antenna gain minus the path loss, all quantities in dB.

A mathematical expression for G was derived by fitting simple polynomials to the normalized measured elevation and azimuth patterns separately and then expressing the gain in general as the product of these two polynomials. The result is the expression

$$G = 13.8\,(1 + 0.104\,\theta - 0.0143\,\theta^2)(1 - 0.000288\,\phi^2)\ \text{dBi}.$$

The two polynomials separately are accurate to about 0.1 dB over their range of coverage (0 to 10 degrees in elevation and -30 to 30 degrees in azimuth).

The elevation angle of an aircraft at altitude h kilofeet and range r nmi, for a 4/3 earth radius sphere, can be computed from the formula

$$\theta = 9.43\,(h/r - 0.000662\,r)\ \text{degrees}.$$

This is the result of applying the series expansions for the elementary angle functions to a readily derived trigonometric formula for the elevation angle. It is accurate to about 0.1 degrees for elevation angles in the range 0 to 10 degrees.

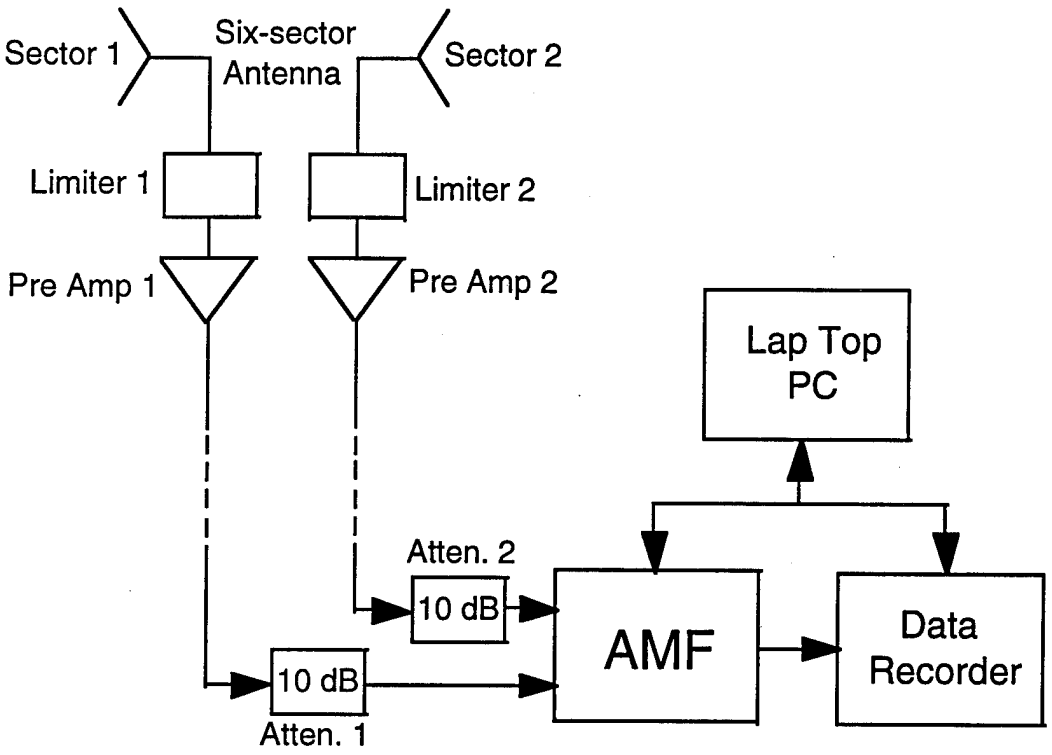

Figure 21. Block diagram of data collection equipment.

APPENDIX C: THE EN-ROUTE LINK BUDGET

The proposed link budget for the en-route stations equipped with a six-sector antenna is as follows in Table 2.

Table 2. En-Route Link Budget

Transmit Power (dBm)	54.0 (250 W)
Transmit gain (dBi)	0.0
Path loss (dB)	-144.5 (200 nmi)
Receive gain (dBi)	14.0 (6-sector antenna)
Circ. & filter loss (dB)	-1.0
Receive power (dBm)	-77.5
Det. threshold (dBm)	-88.0
Margin (dB)	10.5

The margin allows for differences between the nominal and actual gain of the aircraft antenna, for propagation-path variations, and for lower power transponders (the minimum requirement is 48.5 dBm).

APPENDIX D: ANTENNA PERFORMANCE ON A ROCKING BUOY

Ocean buoys have been proposed as sites for GPS Squitter 'ground' stations to provide surveillance of oceanic air routes. Communication back to the ATC system on shore would be carried by a satellite link. To make efficient use of resources, the surveillance antenna would likely be some form of multisector antenna. Its greater range performance, compared with an omnidirectional antenna, permits fewer buoys to be used.

This application imposes the very significant uncertainty of how the combination of the buoy motion and the dynamically varying shape of the reflecting sea surface affects the surveillance performance. The pitching of the buoy has the direct effect on link margin of sweeping the antenna beam, with its narrow elevation beamwidth, up and down through the radio line of sight to the aircraft, causing periodic fading. Additionally, in heavy seas, buoy heave can carry the antenna below the wave crests, causing periodic signal blockage. A third type of fading is caused by the time varying multipath component of the received signal, arriving via reflection from the sea surface. It interferes coherently with the direct signal, and so can reinforce it or weaken it, depending on its relative phase. The geometry is illustrated in Figure 22.

The fact that oceanic routes do not require frequent position updates helps mitigate these problems. The system requirements are more tolerant of breaks in connectivity. The key questions are, how big are the gaps and how does this affect the ATC system.

This Appendix describes the simulation method developed to investigate the first of these questions and presents examples of its results in the form of the temporal statistics of the effective antenna gain.

D.1 MODEL OF SIGNAL PATH

The propagation model has three elements. They are 1) a mathematical description of the surface profile for different sea states, 2) a determination of the resulting heave and pitch of the buoy so that the location and orientation of the antenna with respect to the sea surface can be evaluated as functions of time, and 3) the calculation of the resulting effective gain in the direction of the target aircraft, taking into account the coherent interference from the multipath component reflected from the sea surface.

D.1.1 Wave Spectrum and Buoy Motion

Sea state data derived from motion measurements of moored weather monitoring buoys are available from NOAA. An example, the wave amplitude spectrum, measured on a buoy moored in the open waters of the Gulf of Mexico, is presented in Figure 23. Its narrow unimodal shape is typical of open ocean wave motion.

An explicit time domain sample of the wave amplitude can be synthesized from its spectrum by first using a Gaussian random number generator, weighted by the measured spectrum, to create a frequency domain sample of the wave amplitude and then calculating its Fourier transform. For this, the reasonable assumption can be made that the phases of the different frequency domain components are independent. The corresponding sample of the wave slope is then given simply by multiplying the frequency domain sample of the wave amplitude by the gravity-wave wave number before calculating its Fourier transform. The wave number is given by $(2\pi f)^2/g$, where f is the

frequency and g is the gravitational acceleration. If we assume that all the frequency components of the wave motion move in the same direction, a reasonable assumption for a high sea state in the open ocean, only positive frequencies need be considered.

To transform the wave motion functions into buoy motion functions, one can take advantage of the fact that for the higher sea states of interest for this investigation, the roll-off of the mechanical response function of the 'discus' buoy type likely to be used occurs at a frequency of around 0.5 Hz [4], substantially greater than the peak of the wave amplitude spectrum. (The spectral peak for the moderate sea state illustrated in Figure 23 occurs at 0.14 Hz, and higher sea states would have an even lower peak frequency.) This means that the buoy heave and pitch are essentially the same functions of time as the wave amplitude and slope.

A multiplicity of independent time domain samples of the heave and pitch can be generated in the way described by simply repeating the process, starting with independent applications of the Gaussian random number generator weighted by the same wave amplitude spectrum. They are each samples of the random process defined by the given spectrum.

Figure 24 shows time domain samples of the heave and pitch evaluated from the wave spectrum of Figure 23 in the manner described. The derivation of the corresponding effective antenna gain, also shown, is explained below.

The wave spectrum likely to be of greatest interest for this application is the spectrum of the fully developed sea state. This sea state is reached when the wind holds steady for a long time and the fetch is very large. Then the phase velocity at the spectral peak steadily increases until it becomes commensurate with the wind speed, after which it stays constant. In the process, the wave amplitude also rises until it reaches a limiting value characteristic of the wind speed. (This is not the case for the spectrum shown in Figure 23, which, since the phase velocity at the spectral peak is about 11 m/s, evidently was generated by a wind stronger than the one blowing at the time and location the spectrum was measured. Either the wind had subsided by the time of the measurement, or the generating wind was blowing elsewhere.)

Oceanographers have concocted a mathematical expression for the wave amplitude spectrum of the fully developed sea state. When the phase velocity at the spectral peak is exactly equal to the wind speed, the more general expression [5] reduces to

$$S(f) = f^{-5}\Gamma(f/f_p),$$

where f_p is the frequency at the spectral peak and the shape function $\Gamma(x)$ takes the form

$$\Gamma(x) = 3.705 \times 10^{-4}\, x \exp(-x^{-4})\, 1.7^{\exp\left[-(x-1)^2/0.128\right]}.$$

This spectrum obeys the convenient scaling law

$$S_2(f) = (T_2 / T_1)^5 S_1(T_2 f / T_1),$$

where $S_n(f)$ is the wave amplitude spectral density of the fully developed sea state of dominant period T_n. The scaling law is accurate over the frequency range containing most of the wave energy [5]. The dominant period is defined as the period corresponding to the frequency of the spectral peak. It is the reciprocal of f_p.

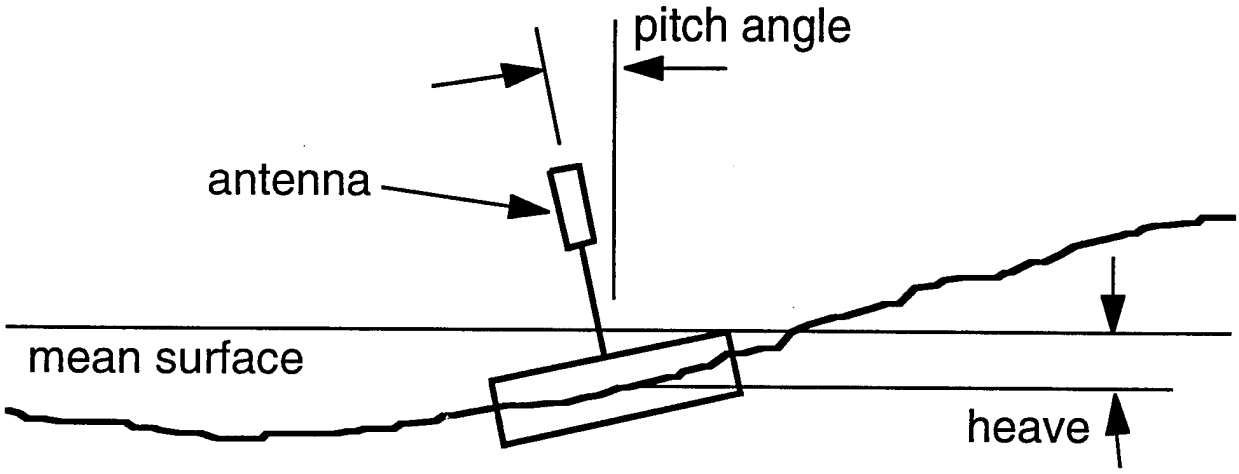

Figure 22. The geometry of the buoy and the water surface.

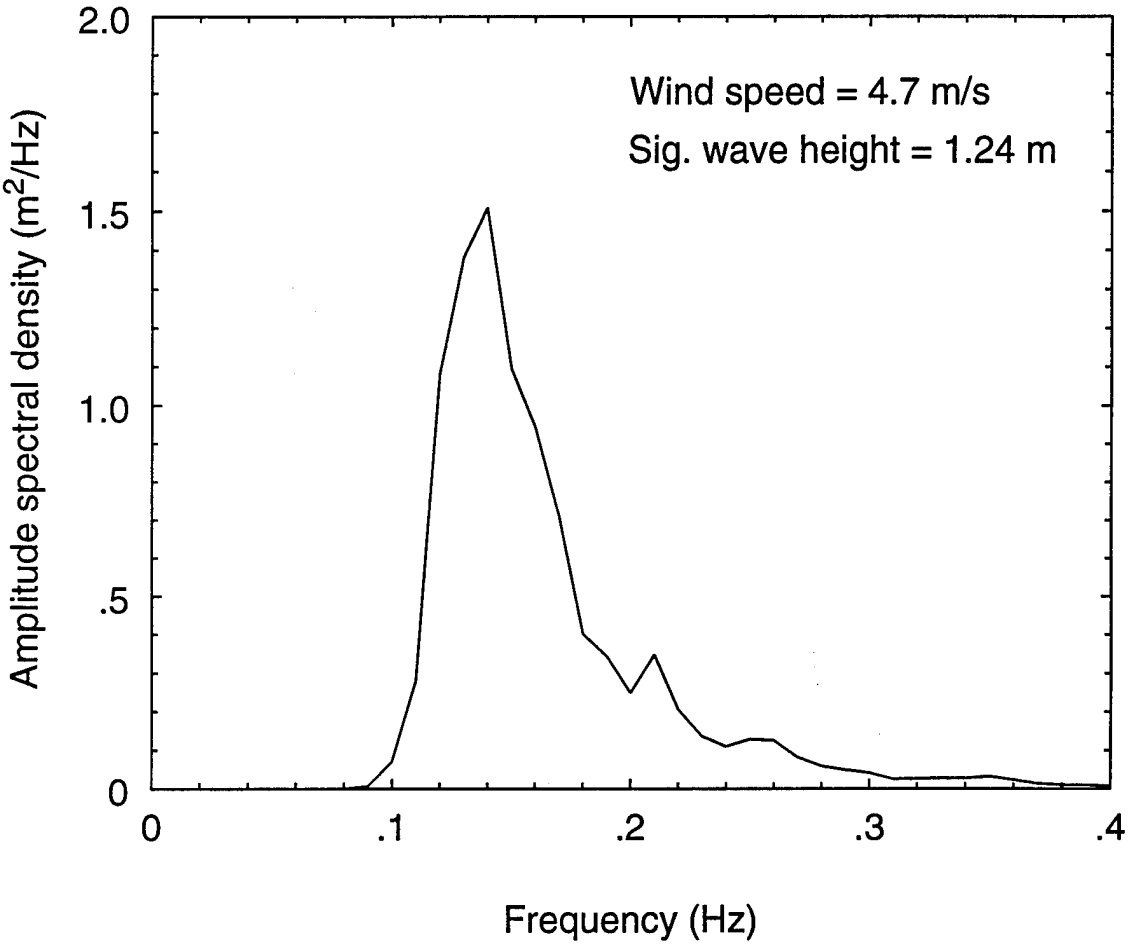

Figure 23. An example of a measured wave amplitude spectrum.

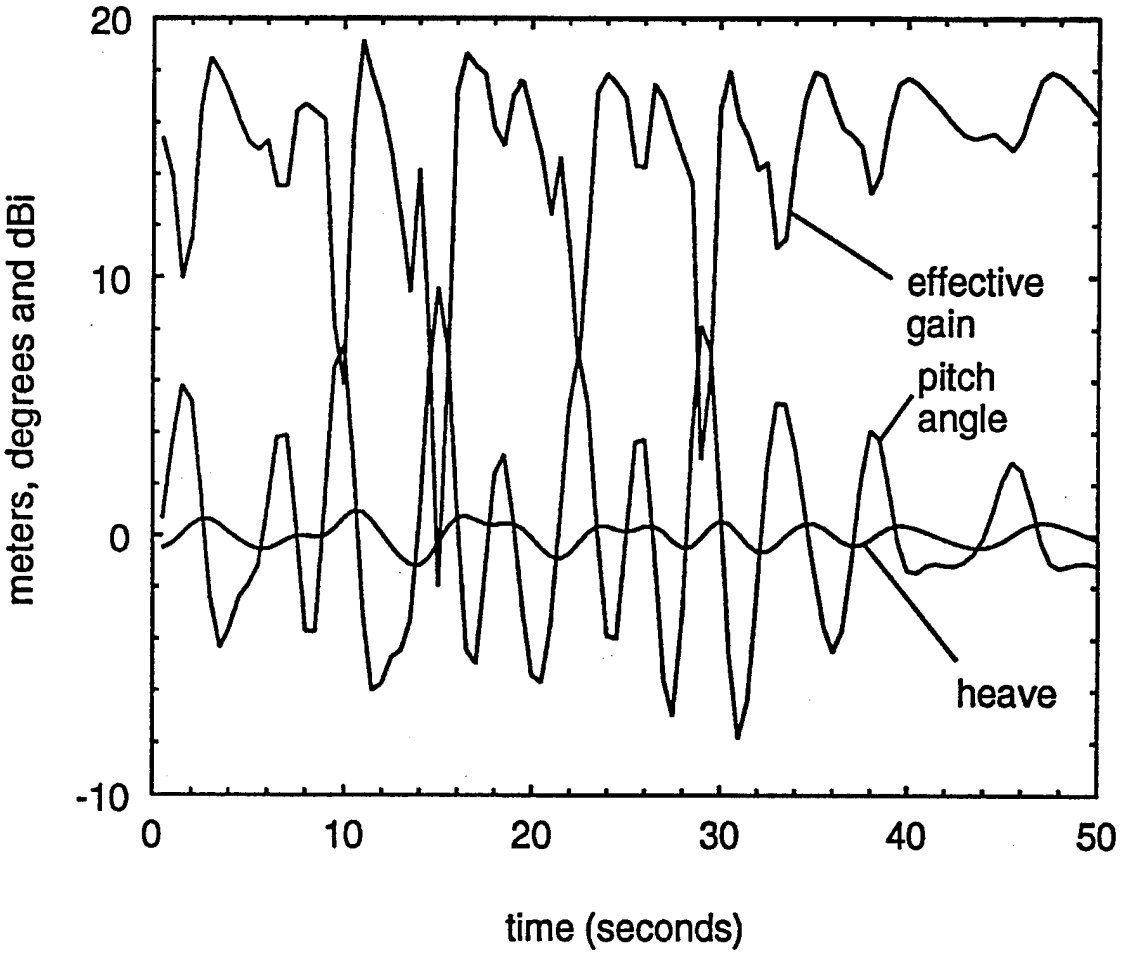

Figure 24. Sample time behavior of pitch angle, heave, and effective gain derived from the heave spectrum.

D.1.2 Effective Gain

The effective gain at any given time is defined as the signal level received by the given antenna, in the presence of the pitch, multipath, and blockage obtaining at that time, relative to the signal level received by an ideal omnidirectional antenna at the same location but with no multipath or blockage. The method adopted here to evaluate it, although not exact, was chosen because a more complete one, such as one involving geometric optics to analyze the scattering from the waves, was judged to be overly elaborate. The likely improvement in accuracy was not sufficient to justify the time needed to implement and verify it.

The method used is as follows:

1) If the antenna is below the general level of the wave crests, the assumption is made that no signal gets through and therefore that the effective gain in dBi is negative infinity.

2) If the antenna is above the general level of the wave crests, the assumption is made that some signal gets through and it is evaluated by combining coherently the direct signal and the multipath signal, taking into account their relative phase and the different antenna gains in the two directions at which the signals arrive at the antenna. The given pitch angle and heave of the buoy, the elevation angle of the transmitting aircraft and the measured gain pattern of the antenna are all be involved in this evaluation. Reflection of the multipath signal from the sea surface is assumed to take place at a horizontal plane at the general level of the wave crests and the reflection is assumed to be loss less.

3) The effect of waves smothering the antenna was neglected, the assumption being that the antenna is mounted high enough above the water level for this to be a very rare event. The effect of the radome simply being wet is known to be negligible at L band [4].

The justification for using the general level of the wave crests both to determine whether blockage occurs and also to define the shape and level of the reflection plane is that the propagation paths of most interest are those originating from aircraft at great ranges, and which therefore arrive at the antenna with small grazing angles relative to the average sea surface. For such paths, the onset of blockage occurs approximately at the time the antenna sinks below the general level of the wave crests. In addition, a well known result of many propagation studies over the years is that at low grazing angles, even very rough surfaces reflect like smooth ones and that the reflection is then nearly perfect.

The final modeling decision to be made is how to define the general level of the wave crests. Oceanographers, faced with the same problem, have developed the concept of the 'significant wave height'. This is a quantity which can be evaluated mathematically from the measured spectrum and which also is closely equal to the average height of the waves estimated by visual observation [6]. Since an L band eye, were it to exist, with its 1-foot operating wavelength, would closely agree with the human eye about the average height of the large waves, this is clearly the appropriate measure to be used here for the general level of the wave crests.

The mathematical definition of the significant wave height is that it is twice the rms wave height or four times the rms wave amplitude. (Wave height is the crest to trough measure of

vertical wave dimension; wave amplitude is the crest to mean measure.) For a narrow wave spectrum, significant wave height is also the average height of the highest 1/3 wave maxima.

D. 2 RESULTS

As is the case for other communication links, the most significant measure of performance here is probably the percentage of the time, over an extended period of operation, that the effective gain in the direction of the aircraft remains below a threshold of, say, 8 dBi for 10 seconds or more. A compilation of such time gap statistics, using different gain thresholds and different time gap durations, provides information needed to assess the surveillance reliability of the ground station.

Figures 25 and 26 show examples, using the spectrum shown in Figure 23, for the cases that the line of sight to the transmitting aircraft is perpendicular and parallel respectively to the crest line of the waves. The two cases differ because in the first case buoy motion sweeps the flat fan beam of the antenna up and down through the line of sight and in the second, the dominant behavior is twisting of the beam. Yet another assumption used to generate these results is that the water waves are plane waves, implying that the buoy pitches only in one direction as the waves sweep by.

These results indicate that for this sea state, the chance of not getting an effective gain of at least 16 dBi sometime in any 10 s time period is essentially zero. They also show that 50% of the time, the effective gain is at least 16 dBi. These two measures taken together imply that if the squitters are emitted by the aircraft at the rate of about one per second, then the chances are very high that at least one will be received by the 'ground' station in any 10 s time period.

However, this sea state (about 3) is not very high. Figures 27 through 29 show the spectrum and the corresponding time gap statistics for a much higher one. They use the formula defined above for the fully developed spectrum of a sea state having a wave period of 12 s. The corresponding significant wave height is 7.0 m and the sea state is 7. The link performance is accordingly much more marginal. On the other hand, in the Gulf of Mexico, the sea state is lower than this on average for all but one or two hours per year [4].

These results illustrate the kind of performance statistics that the software can generate. No definitive conclusions about communication link performance should be drawn from them, however, until the effects are explored of varying the different parameters over their appropriate ranges of values.

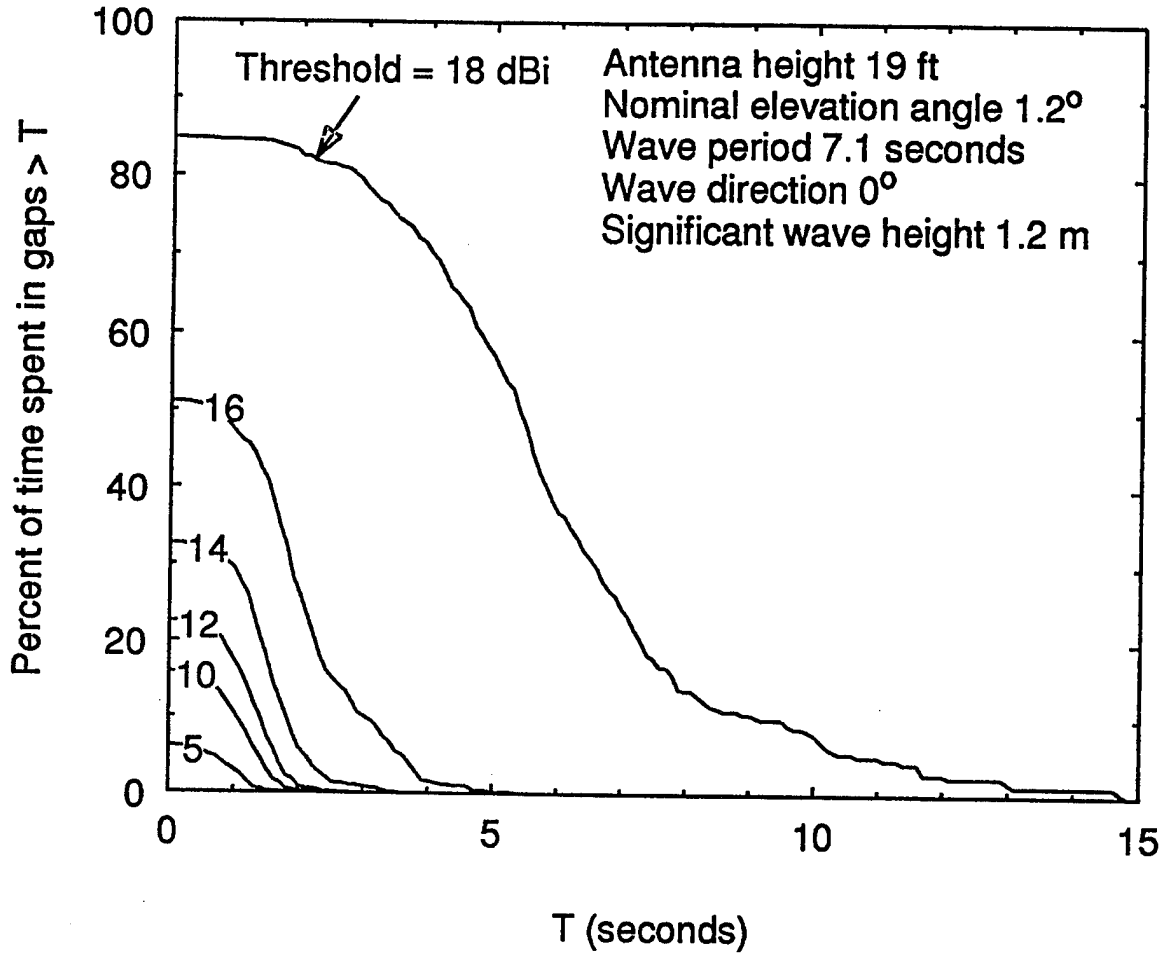

Figure 25. Time gap statistics for the wave spectrum of Figure 23 for a wind-aligned line of sight. (The wave crest line lies perpendicular to the line of sight.)

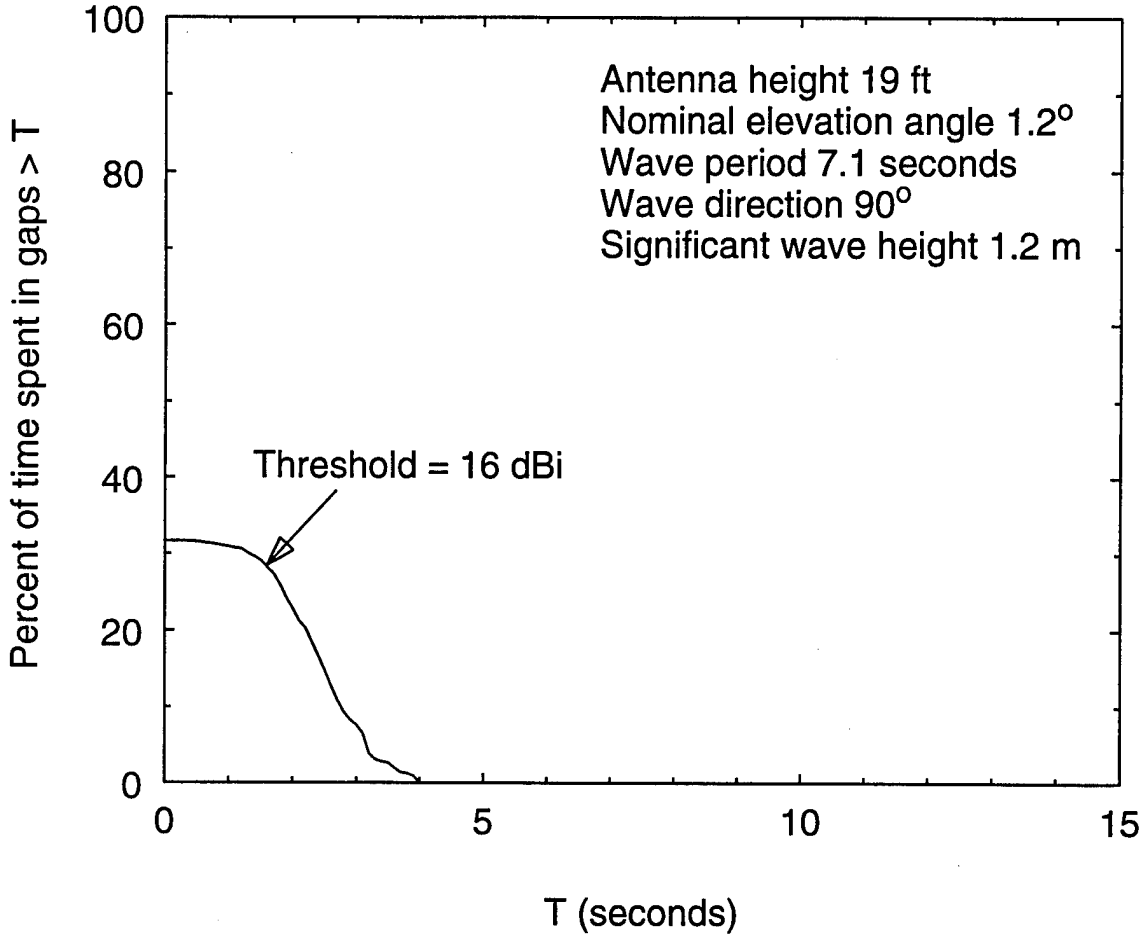

Figure 26. Time gap statistics for the wave spectrum of Figure 23 for a cross-wind line of sight. (The wave crest line lies parallel to the line of sight.)

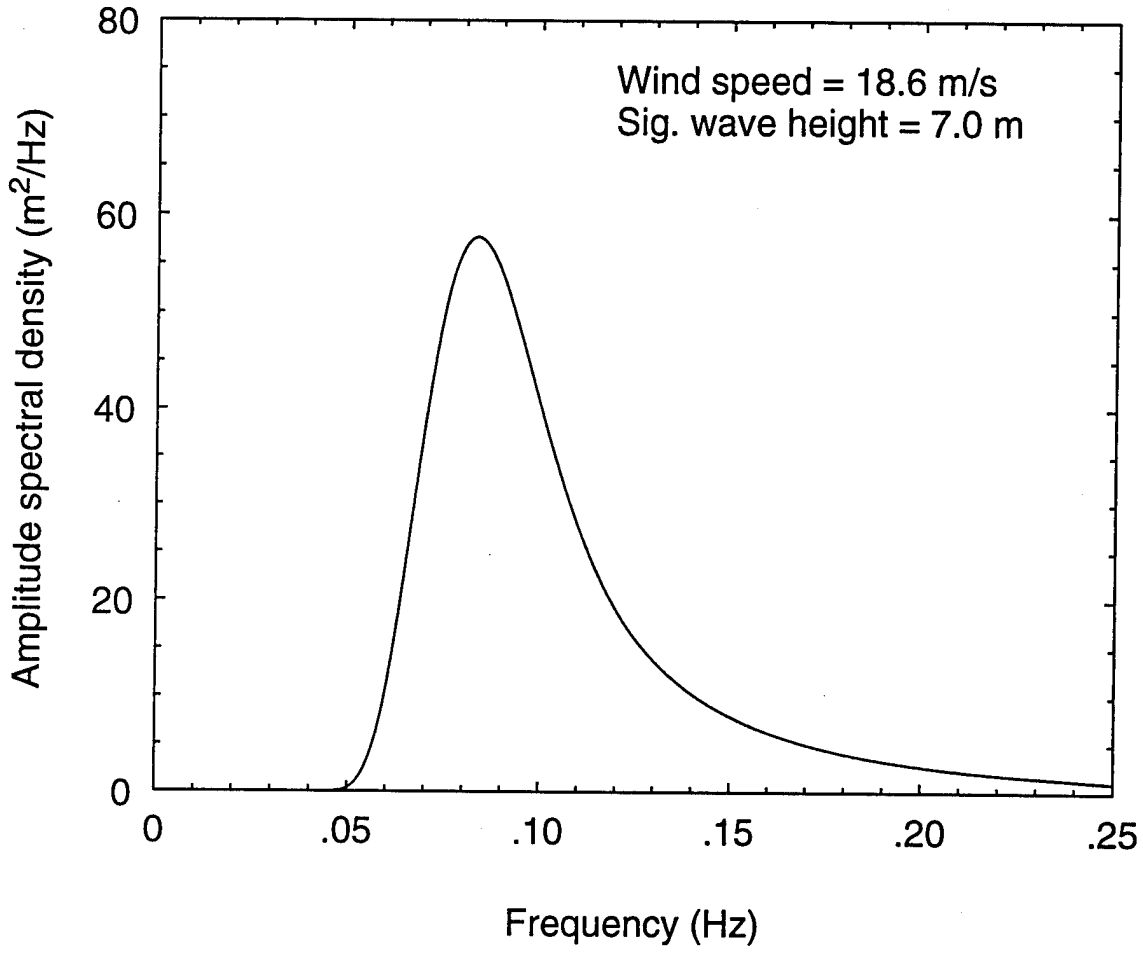

Figure 27. The mathematical wave spectrum of a fully developed sea state having a dominant wave period of 12 s.

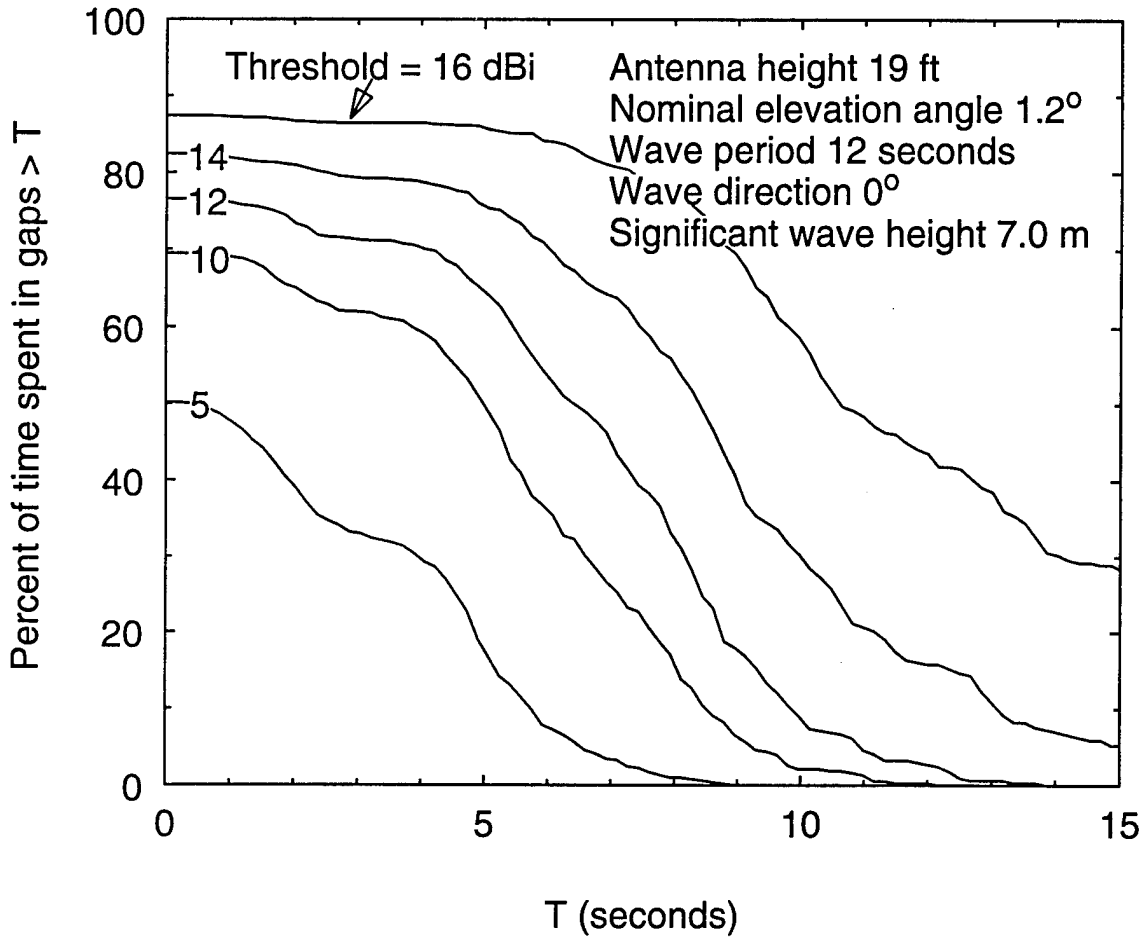

Figure 28. Time gap statistics for the fully developed wave spectrum of Figure 27 for a wind-aligned line of sight. (The wave crest line lies perpendicular to the line of sight.)

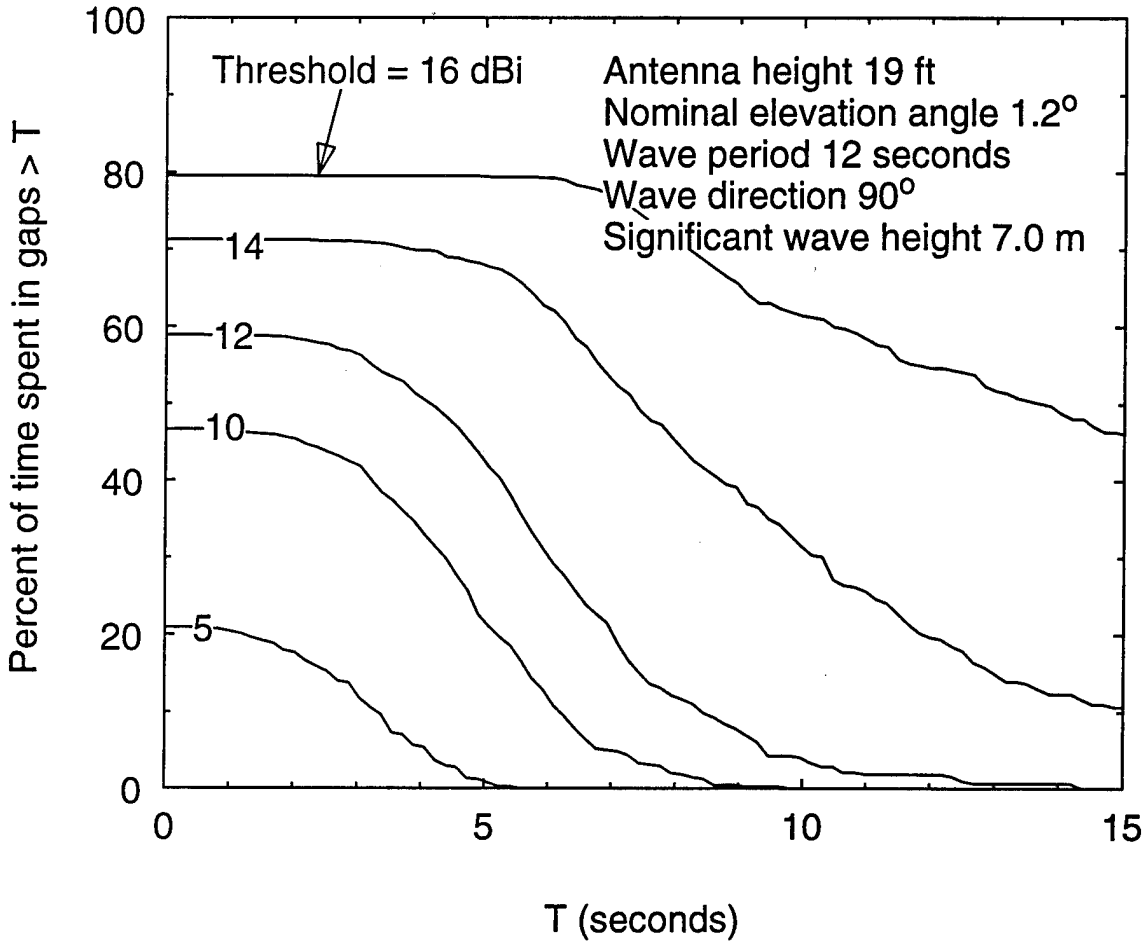

Figure 29. Time gap statistics for the fully developed wave spectrum of Figure 27 for a cross-wind line of sight. (The wave crest line lies parallel to the line of sight.)

REFERENCES

[1] V. A. Orlando, "ADS-Mode S: Initial System Description," MIT Lincoln Laboratory Project Report ATC-200, 2 April 1993.

[2] E. T. Bayliss, R. E. Boisvert, M. L. Burrows and W. H. Harman, "Aircraft Surveillance Based on GPS Position Broadcasts from Mode S Beacon Transponders," in GPS-94, Proceedings of the Institute of Navigation, Salt Lake City, UT, 22-24 September 1994.

[3] S. I. Altman and P. M. Daly, "The Enhanced Airborne Measurement Facility Recording System," MIT Lincoln Laboratory Project Report ATC-228, 31 January 1995.

[4] R. Dagnall, National Data Buoy Center, Stennis, MS, private communication.

[5] G. J. Komen *et al., Dynamics and Modeling of Ocean Waves,* Cambridge University Press, 1994, p. 183ff.

[6] G. J. Komen *et al., op. cit.* p. 34.